N95-28471

TENSION FRACTURE OF LAMINATES FOR TRANSPORT FUSELAGE PART I: MATERIAL SCREENING[1]

T. H. Walker, W. B. Avery, L. B. Ilcewicz
Boeing Commercial Airplane Group
Seattle, Washington

C. C. Poe, Jr., and C. E. Harris
NASA Langley Research Center
Hampton, Virginia

NASA 59-05 51349 P-41

ABSTRACT

Transport fuselage structures are designed to contain pressure following a large penetrating damage event. Applications of composites to fuselage structures require a database and supporting analysis on tension damage tolerance. Tests with 430 fracture specimens were used to (1) identify critical material and laminate variables affecting notch sensitivity, (2) evaluate composite failure criteria, and (3) recommend a screening test method. Variables studied included fiber type, matrix toughness, lamination manufacturing process, and intraply hybridization. The laminates found to have the lowest notch sensitivity were manufactured using automated tow placement. This suggests a possible relationship between the stress distribution and repeatable levels of material inhomogeneity that are larger than found in traditional tape laminates. Laminates with the highest notch sensitivity consisted of toughened matrix materials that were resistant to a splitting phenomena that reduces stress concentrations in major load bearing plies. Parameters for conventional fracture criteria were found to increase with crack length for the smallest notch sizes studied. Most material and laminate combinations followed less than a square root singularity for the largest crack sizes studied. Specimen geometry, notch type, and notch size were evaluated in developing a screening test procedure. Traditional methods of correcting for specimen finite width were found to be lacking. Results indicate that a range of notch sizes must be tested to determine notch sensitivity. Data for a single small notch size (0.25 in. diameter) was found to give no indication of the sensitivity of a particular material and laminate layup to larger notch sizes.

INTRODUCTION

Boeing's program for Advanced Technology Composite Aircraft Structure (ATCAS) is studying manufacturing and performance issues associated with a wide body commercial transport fuselage (Ref. 1). Tension damage tolerance and pressure containment are major technical issues to solve for fuselage structures. Although composites are generally thought to have excellent tension properties, there is limited data on the performance of configured composite shell structures with large through-penetrating damage and subjected to combined load conditions, including pressure. A collaborative effort between Boeing and NASA is committed to collecting a database and solving the technical challenges associated with composite fuselage damage tolerance.

---

[1] This work was funded by Contract NAS1-18889, under the direction of J. G. Davis and W. T. Freeman of NASA Langley Research Center.

PRECEDING PAGE BLANK NOT FILMED
PAGE 746 INTENTIONALLY BLANK

During the last year, much of the work in ATCAS has concentrated on local cost and weight optimization of crown panels (Ref. 2). The minimum gage structures that constitute crown panels in ATCAS are characteristic of up to 70% of the fuselage surface area. Depending on material selection and design details, both hoop and axial tension damage tolerance can be design drivers for the ATCAS crown panels. The crown local optimization task which is the subject of this paper involved the collection of a tension fracture database for candidate skin materials. During the course of achieving this task, a process-related characteristic was found to increase tension fracture performance of automated tow-placed laminates. As discussed at the start of Reference 2, the improved fracture strength lead to projections for significant reductions in structural cost and weight.

Most of the published tension fracture work performed to date has concentrated on relatively small notches, having sizes less than 1 in. (see Ref. 3 for a review of work up to 1985). A previous NASA-funded program at Boeing included tests with larger cracks, characteristic of transport fuselage damage tolerance criteria (Ref. 4). Some modification to classical fracture analyses (e.g., addition of a semi-empirical characteristic dimension in failure criteria or a change in the order of crack tip singularity) was used in most past studies to predict tension fracture in composite laminates. More recent work has considered the effects of pre-catastrophic damage growth on stress redistribution at the crack-tip. Results from both small and large cracks indicate that numerous variables affect tension fracture, including laminate thickness, ply stacking sequence, fiber type, and matrix type.

With the multitude of variables affecting tension fracture for composite materials (Ref. 5), it is desirable to screen performance at the coupon level. One material screening test, used extensively by the aerospace industry over the past few years, is uniaxial tension loading of a notched specimen having a 0.25 in. diameter open hole. Little work has been performed to indicate that test results from this narrow specimen are suitable for material screening of tension fracture for transport fuselage damage tolerance. In order for the test to have qualitative meaning, there needs to be an experimental correlation established between small and large notch data. Supporting analyses are also needed to quantify fuselage damage tolerance based on specimen data available during preliminary design.

The current paper reviews the "small notch" ATCAS tension fracture specimen database collected for ten candidate crown skin materials. The test matrix was designed to assess uniaxial tension fracture for layups and thicknesses characteristic of the skins for stiffened fuselage panel design concepts. Both traditional tape and tow-placed laminates were evaluated. Test results were analyzed to assess critical material variables such as fiber type, matrix type, and intraply hybridization. Three different notch types were studied; machined cracks, drilled holes, and through-penetrations created by subjecting the laminate to an impact event with a sharp blade. In addition to characterizing material performance, the database served three other purposes. First, there was a desire to confirm the equivalence of laminates fabricated by automated tow placement and hand layup using tow and tape material forms, respectively. Second, tension fracture analyses and failure criteria were evaluated for a range of crack lengths from 0.25 in. to 5.0 in. Third, a suitable method for material screening was derived based on experimental and analytical results.

The following text is divided into four main sections. The first section gives a detailed account of specimen fabrication and test procedures. The second section discusses trends in experimental results. Statistical data analysis was performed to judge if the trends in material performance for small cracks are indicative of those for the largest cracks tested. The accuracy of a number of failure criteria for predicting notched strength is covered in the third section. This includes a review of the importance of the scale of material inhomogeneity and order of crack tip singularity. A comparison of results for width-to-notch-size ratios of 2 and 4 is used to discuss the validity of analysis methods for correcting fracture results for finite specimen width. In the final section, recommended test procedures for fuselage material screening are discussed.

EXPERIMENTS

Test Matrix

The test matrix of 430 coupons is shown in Figure 1. Laminates were made from ten materials. The first two materials are the primary fiber and matrix candidates, IM6[2]/937A[3] and AS4[4]/938[5], both in tape form (937A and 938 are resin systems nearly identical to 3501-6[6]). At the time the test matrix was formulated, tow and tape laminates consisting of the same constituents and volume fractions were expected to have nearly equivalent performance. The tape laminates fell into three categories: (1) angle- and cross-ply laminates (0/90, +45/-45, and +30/-30) as building blocks for predictive method development; (2) quasi-isotropic and other potential crown laminates (Quasi, Crown1, and Crown2) for evaluation of realistic performance; and (3) the Crown1 laminate rotated 15° and 30° with respect to the crack and loading orientations (Crown1 + 15, Crown1 + 30) for validation of the generality of predictive models. Other variables considered were notch size, notch type, and specimen-width-to-notch-size ratio (*W/2a*). Notch sizes ranged from 0.25 to 5.00 inches, while notch types included holes, machined cracks, and penetrations (i.e., cracks created by penetrating the laminate with a chissle-like impactor). The latter notch type was included to evaluate the effects of the damage zone created by a realistic penetration event, since clean cracks, analogous to fatigue cracks in metals, do not form in composites. *W/2a* ratios of 2 and 4 were included.

A single laminate type (Crown1) was made from each of the remaining eight materials to allow limited comparisons with the two primary fiber and matrix candidates. The Crown1 laminate was the most likely candidate for the skin laminate in the fuselage crown when the testing was defined. Specimens for these limited comparisons were restricted to a $W/2a = 4$.

The IM7[7]/8551-7[8] was included as a representative toughened material system. Since tow-placement was the selected manufacturing process for the crown, AS4/938 tow was included to evaluate process-induced performance changes from the tape form. In combination with the S2[9]/938 tow, it also served as material endpoints for comparison with the intraply hybrids, which comprise the final five materials.

Intraply hybrids, as discussed in this paper, are materials with tows of more than one fiber type combined in a repeating pattern within each individual ply, as shown in Figure 2. These hybrid materials appeared attractive due to potential tension fracture performance improvements and reduced material costs. The materials tested in the current work were an extension of the fiberglass buffer strip

---

[2] IM6 is a graphite fiber system produced by Hercules, Inc.

[3] 937A is a resin system produced by ICI/Fiberite.

[4] AS4 is a graphite fiber system produced by Hercules, Inc.

[5] 938 is a resin system produced by ICI/Fiberite.

[6] 3501-6 is a resin system produced by Hercules, Inc.

[7] IM7 is a graphite fiber system produced by Hercules, Inc.

[8] 8551-7 is a resin system produced by Hercules, Inc.

[9] S2 is a glass fiber system produced by Owens-Corning Fiberglas, Corp.

concept, which has been widely shown to improve tension fracture strength (e.g. Ref. 6, 7), to multiple directions and a material lamina scale. The advent of the tow-placement process allows such materials to be created with little impact on the manufacturing cost. Any significant performance improvement would result in a reduction of the total material requirement, thereby reducing the structural weight, total material costs, and manufacturing costs. In addition, the use of fiberglass as the hybridizing fiber would result in lower material unit costs, since it would replace higher-cost graphite fiber, although at a slight density penalty.

Notch Type ►		Open Hole			Machined Slit							Penetration
Notch Size ►		0.25	0.50	0.875	0.25	0.50		0.875		1.75	2.50	5.00	0.875
Material	Width / Length / Laminate	1.00 12.0	2.00 12.0	3.50 12.0	1.00 12.0	1.00 12.0	2.00 12.0	1.75 12.0	3.50 12.0	3.50 12.0	10.00 30.0	10.00 30.0	3.50 12.0
AS4/938 Tape	0/90		3		3	3	3	3	3		2		
	+45/-45		3		3	3	3	3	3		2		
	+30/-30		3		3	3	3	3	3		2		
	Quasi		3		3	3	3		3				3
	Crown1		3		3	3	3	6	3	3	2	2	3
	Crown1 + 15		3		3	3	3		3				
	Crown1 + 30		3		3	3	3		3		2		
	Crown2		3		3	3	3		3				3
IM6/937A Tape	0/90		3		3	3	3	3	3		2		
	+45/-45		3		3	3	3	3	3		2		
	+30/-30		3		3	3	3	3	3		2		
	Quasi		3		3	3	3		3				3
	Crown1		3		3	3	3	6	3	3	2	2	3
	Crown1 + 15		3		3	3	3		3				
	Crown1 + 30		3		3	3	3		3		2		
	Crown2		3		3	3	3		3				3
IM7/8551-7 Tape	Crown1				3		3		3		2	2	4
AS4/938 Tow	Crown1	3		3	3				3		2		3
S2/938 Tow	Crown1	3		3	3				3		2		3
Hybrid 1 / 938	Crown1			3	3						2		3
Hybrid 2 / 938	Crown1	3							3		2		3
Hybrid 3 / 938	Crown1			3	3						2		3
Hybrid 4 / 938	Crown1	3							3		2		3
Hybrid 5 / 938	Crown1	3		3	3				3		2		3

Layup Designations			
0/90	[0/90]2S	Crown1	[+45/90/-45/0/+30/-30/0/-45/90/+45]
+45/-45	[+45/-45]2S	Crown1 + 15	[+60/-75/-30/+15/+45/-15/+15/-30/-75/+60]
+30/-30	[+30/-30]2S	Crown1 + 30	[+75/-60/-15/+30/+60/0/+30/-15/-60/+75]
Quasi	[+45/90/-45/0]S	Crown2	[+45/-45/0/90/+30/-30/0/90]S

Hybrid Material Definitions		
Hybrid No.	Hybridization	Repeat Unit Width
1	75% AS4, 25% S2	4 Tows
2	50% AS4, 50% S2	4 Tows
3	50% AS4, 50% S2	12 Tows
4	75% AS4, 25% S2	12 Tows
5	75% AS4, 25% T1000	12 Tows

Figure 1: Specimen Configurations and Number of Replicates for Tension Fracture Testing

The configuration of the intraply hybrid materials considered in the current program are detailed in Figure 2. AS4/938 was the baseline tow. In Hybrids 1 through 4, the AS4 was combined with a low-stiffness, high-strain fiber, S2 fiberglass. In Hybrid 5, AS4 was combined with high-stiffness/high-strain graphite fiber, T1000[10]. Variables evaluated for these materials were notch size and type, hybridization percentage, and repeat unit width.

[10] T1000 is a graphite fiber system produced by Toray Industries, Inc.

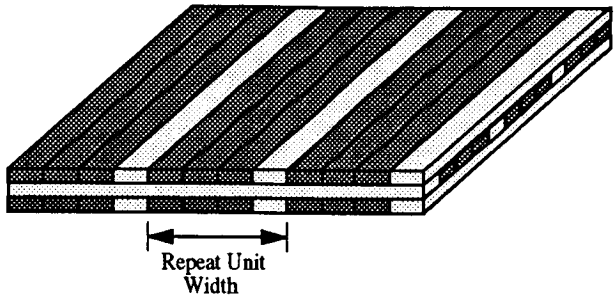

Designation	Base Mat'l Tow	Hybridizing Mat'l Tow	Repeating Pattern	Repeat Unit Width
Hybrid #1	AS4/938	S2/938		0.38 in.
Hybrid #2	AS4/938	S2/938		0.38 in.
Hybrid #3	AS4/938	S2/938		1.10 in.
Hybrid #4	AS4/938	S2/938		1.10 in.
Hybrid #5	AS4/938	T1000/938		1.10 in.

Figure 2: Intraply Hybrid Material Description

For the AS4/S2 hybrids, an eight run designed experiment was used to evaluate (1) notch sizes of 0.25 and 0.875 inches, (2) notch types of holes and cracks, (3) hybridizing percentages of 25% and 50% S2-glass, and (4) repeat unit widths of 4 and 12 tows. Within this designed experiment, the Crown1 layup and a *W/2a* of 4 remained constant for all specimens. Additional tests were conducted outside the designed experiment for 2.5 inch cracks and 0.875 inch penetrations. A fully crossed matrix of the above notch variables was tested for Hybrid 5, which was a 75%/25% combination of AS4 and T1000, respectively, with a 12 tow repeat unit.

All laminates in the test matrix were fabricated from material with a fiber volume of approximately 57% (corresponding to a resin content of 35% for graphite/epoxy systems). The fiber tows used in all tape materials were 12K. To maintain approximately equal tow spread for all intraply hybrid fiber types, 6K tows of AS4 and 12K tows of T1000 were used, as was 20 end 750 yd./lb. S2-glass.

Panel Fabrication

A single panel was manufactured for each unique combination of material and laminate type. The tape panels were fabricated from 12 inch wide prepreg tape using standard hand layup techniques. The tow-placed panels were fabricated on the Hercules 6-axis fiber placement machine using a 12-tow Band Cut and Add head. All panels were autoclave cured at 350°F. Nominal cured ply thickness for both tow and tape materials was 0.0074 in. Through-transmission ultrasonics was used to non-destructively inspect each panel after cure to ensure laminate quality. Measurements of laminate thickness indicated that all panels fabricated were within specified limits.

Specimen Machining

The coupons were cut to slightly oversized dimensions using a band saw, then sanded to final dimensions. A 125 surface finish was designated for all cut edges. The open holes were created using tapered drills. Cracks were created by drilling two 0.070 inch diameter holes at the crack tip locations, then connecting them using an abrasive waterjet cutter. X-ray inspection was used to assess machining-induced damage. Specimen thickness, width, and notch size were measured prior to testing.

The 10 in. x 30 in. coupons were tabbed with 10 in. x 3 in. tabs on both sides of each end to insure against failure in the grips. The 100% S2-glass and the S2-glass hybrid coupons utilized tabs fabricated from E-glass/5208[11] 8HS prepreg with a $[0/45/0]_s$ stacking sequence. The AS4/938, IM6/937A, IM7/8551-7, and AS4/T1000 hybrid test specimens utilized tabs fabricated from T300[12]/5208 plain weave fabric prepreg with a $[0]_n$ stacking sequence. All tabs had a nominal thickness of approximately 0.07 inches, and were bonded to the test specimens with a 0.010 inch thick 250°F cure film adhesive. The test specimens and tabs were prepared for bonding by lightly grit blasting the bonding surfaces, followed by a solvent wipe to remove any loose material.

Test Procedures

The through-penetration damages were created by impacting individual specimens in an impact tower. The specimen support fixture is illustrated in Figure 3, and consists of a 0.50 inch steel plate with a 5.0 in. x 2.5 in. cutout. Specimens were held with clamps at each end of the specimen to prevent specimen rebound during impact. The test fixture approximates simply-supported boundary conditions. An instrumented impact tower was used to perform the penetration event. A steel blade with a width and thickness of 0.875 in. and 0.060 in., respectively, and a 45° thickness-taper at the tip was dropped at a velocity of 12.5 ft./sec. The weight of the impactor was approximately 13.6 lbs., thus producing an impact energy of 400 in.-lbs. Force, energy, and deflection versus time were recorded by a data acquisition system and digitally stored. After impact, the damage in each specimen was assessed ultrasonically using the pulse-echo time-of-flight technique at a frequency of 5 MHz.

Testing was conducted in two test machines. The 1-in.-wide specimens were tested in a 20 kip test frame, while all others were tested in a 56 kip hydraulic test frame. A displacement rate of 0.125 in./min. was used for the 10-inch-wide coupons, while 0.05 in./min. was used for all other specimens. All tests were conducted at room temperature and ambient humidity.

X-ray radiographs were obtained for one of the three replicates of many of the 1- and 3.5-in.-wide specimen types to document pre-failure damage progression. X-rayed specimens were loaded to between 75 and 90% of the expected failure load prior to inspection, and were subsequently loaded to failure.

Extensometers placed approximately midway between the notch and the loading frame were used to monitor far-field strains during loading. Strain gages were used on some specimens to measure far-field strain, local load redistribution and transverse buckling adjacent to the unsupported edges of the crack. Several tests were recorded on videotape to document failure mechanisms and progression.

---

[11] 5208 is a resin system produced by Narmco Materials, Inc.

[12] T300 is a graphite fiber sytem produced by Toray Industries, Inc.

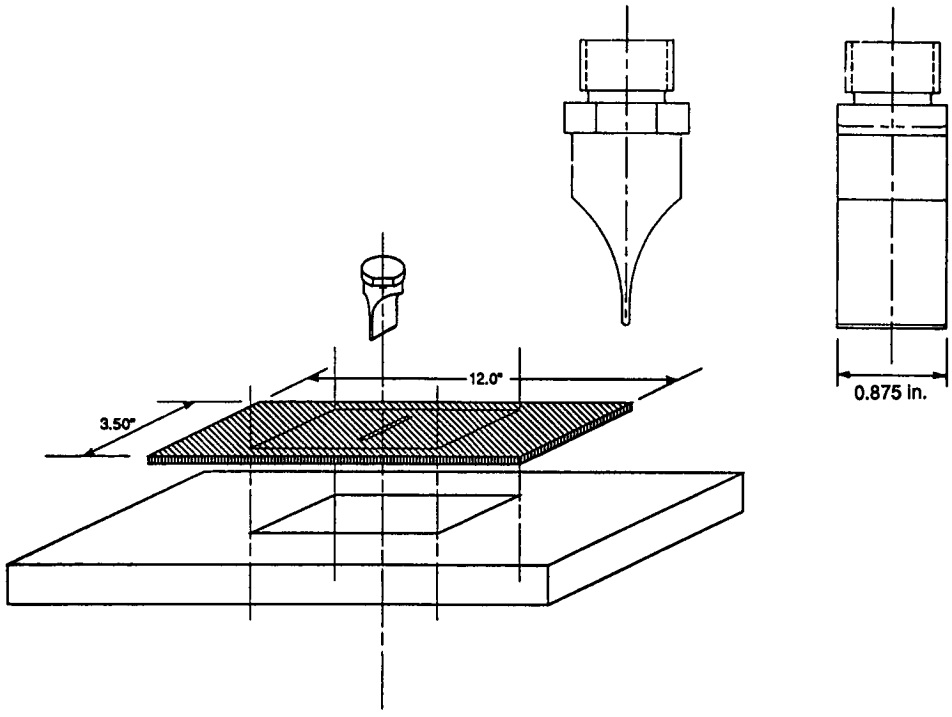

Figure 3: Penetrating Impact Support Fixture

TEST RESULTS

The average nominal failure stress (i.e., failure load ÷ (number of plies * nominal ply thickness)) for each specimen configuration is listed in Figure 4. In the following subsections, the important results are presented and discussed.

Layup

As shown in Figure 5, large variations in fracture strength with layup were observed within each material type. The relationship between layup and notched tensile strength has been shown to be complex (e.g., Refs. 8-13). Certain combinations of ply splitting and delamination that occur at a crack tip can enhance residual strength by effectively reducing the stress concentration. Delaminations that extend to the edge of finite-width specimens, uncoupling plies and allowing them to fail without fiber breaks, however, reduce the residual strength.

The laminates in Figure 5 for each material are shown in order of decreasing axial modulus. It appears that fracture strength tends to increase with increasing modulus. The 0/90 laminates had significantly higher strengths than all other laminates, and a somewhat reduced sensitivity to changes in crack length. Despite relatively low fracture strength of the +45/-45 laminates, this layup was found to be relatively notch insensitive, as seen by comparing results for different crack sizes in Figure 4. This agrees with data presented in Reference 14.

Notch Type ►		Open Hole			Machined Slit							Penetration
Notch Size ►		0.25	0.50	0.875	0.25	0.50		0.875		1.75	2.50	5.00	0.875
Material	Width / Laminate / Length	1.00 / 12.0	2.00 / 12.0	3.50 / 12.0	1.00 / 12.0	1.00 / 12.0	2.00 / 12.0	1.75 / 12.0	3.50 / 12.0	3.50 / 12.0	10.00 / 30.0	10.00 / 30.0	3.50 / 12.0
AS4/938 Tape	0/90		50.80		59.70	34.68	49.94	35.47	49.05		45.63		
	+45/-45		17.74		17.58	11.12	18.30	12.00	17.93		17.45		
	+30/-30		40.93		49.98	31.10	45.38	28.12	35.56		26.44		
	Quasi		43.67		44.70	28.51	39.61		36.30				35.39
	Crown1		36.98		44.68	28.11	41.42	27.35	38.02	18.71	27.90	14.10	35.22
	Crown1 + 15		34.98		41.54	29.42	35.70		31.02				
	Crown1 + 30		35.34		42.49	25.73	34.14		35.82		26.35		
	Crown2		42.43		45.12	29.74	36.49		31.52				38.74
IM6/937A Tape	0/90		70.24		72.97	52.74	68.10	43.79	61.95		57.69		
	+45/-45		17.74		17.28	11.33	18.16	11.91	18.00		18.33		
	+30/-30		48.65		56.66	34.90	51.35	36.00	42.79		35.45		
	Quasi		51.04		62.08	36.98	75.26*		51.11				50.34
	Crown1		42.21		51.95	34.66	46.24	32.08	39.63	27.59	34.64	16.92	43.96
	Crown1 + 15		45.14		53.19	37.55	51.40		38.50				
	Crown1 + 30		46.22		54.53	34.35	46.82		35.22		32.18		
	Crown2		48.56		58.24	37.18	48.56		41.53				53.02
IM7/8551-7 Tape	Crown1				69.68		61.40		53.41		32.23	18.04	43.82
AS4/938 Tow	Crown1	49.87		41.48	50.45				46.33		35.27		44.04
S2/938 Tow	Crown1	51.11		54.44	53.47				52.70		45.05		49.65
Hybrid 1 / 938	Crown1			43.24	52.20						37.81		44.53
Hybrid 2 / 938	Crown1	47.91							48.83		40.35		44.08
Hybrid 3 / 938	Crown1			39.25	51.05						41.12		40.30
Hybrid 4 / 938	Crown1	47.64							46.96		36.61		43.60
Hybrid 5 / 938	Crown1	55.36		44.78	57.17				50.37		41.18		47.89

Layup Designations			
0/90	[0/90]2S	Crown1	[+45/90/-45/0/+30/-30/0/-45/90/+45]
+45/-45	[+45/-45]2S	Crown1 + 15	[+60/-75/-30/+15/+45/-15/+15/-30/-75/+60]
+30/-30	[+30/-30]2S	Crown1 + 30	[+75/-60/-15/+30/+60/0/+30/-15/-60/+75]
Quasi	[+45/90/-45/0]S	Crown2	[+45/-45/0/90/+30/-30/0/90]S

* These data appear in error but no good explanation was found.

Hybrid Material Definitions		
Hybrid No.	Hybridization	Repeat Unit Width
1	75% AS4, 25% S2	4 Tows
2	50% AS4, 50% S2	4 Tows
3	50% AS4, 50% S2	12 Tows
4	75% AS4, 25% S2	12 Tows
5	75% AS4, 25% T1000	12 Tows

Figure 4: Average Nominal Failure Stress Results

Notch Type

The open hole and crack strengths were within approximately 10% of each other. The relative severity varied among the laminates. These results are similar to the small notch results summarized in Reference 3. For the Crown1 laminate that was used for the majority of material comparisons, holes were found to have strengths below those of cracks.

Comparison of the instrumented impact force-displacement results for the through-penetrations revealed significant differences between material types. The slope of the force-displacement curve relates to the plate bending stiffness, and the area under the curve is a measure of the event energy. This event energy is a combination of the energy absorbed by the plate during the penetration event and the energy required to bend the plate. Instrumented impact results for non-penetrating events typically subtract out the plate-bending component. For the case of a through-penetration event, however, the plate rebound energy cannot be measured since the displacement is associated with the impactor.

Force-displacement curves for Crown1 laminates fabricated from AS4/938 tape, AS4/938 tow, IM6/937A tape, and IM7/8551-7 tape are presented in Figure 6. The AS4/938 tow has a higher load than the AS4/938 tape, resulting in an approximately 60% higher event energy. This difference may

be attributed to an increase in damage formed adjacent to the penetration in the tow-placed laminate. This was confirmed by ultrasonic scans.

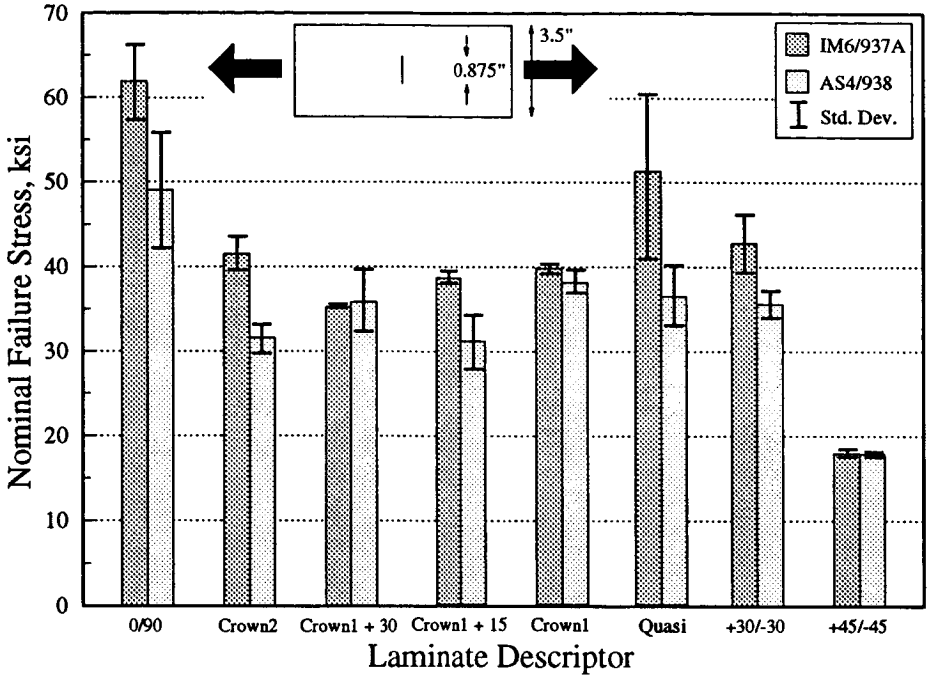

Figure 5: Variation of Fracture Strength with Layup for IM6/937A and AS4/938 Tape

The IM6/937A tape instrumented impact results showed a peak load and total event energy that were 20-25% above that of the AS4/938 tape. The amount of damage area created was similar for the two materials, as might be expected for equivalent resin systems. The energy differences, therefore, might be due to the slightly higher laminate bending stiffness and fiber strengths, both a result of the higher stiffness of the IM6 fiber.

As also shown in Figure 6, penetration of IM7/8551-7 tape resulted in a 40% higher maximum load and a 65% higher total event energy than IM6/937A tape. Ultrasonic scans indicated that damage created adjacent to the penetration was significantly smaller in IM7/8551-7 than in any of the other materials. Possible causes for the energy difference include (a) the slightly higher bending stiffness and fiber strength with the IM7 fiber, and (b) the increased energy absorbed per unit damage due to the higher toughness of 8551-7. Neither of these, though, appear likely to account for a majority of the energy increase. Extension of the crack beyond the net impactor length, however, would require additional fiber failure and associated energy. This scenario is plausible since 8551-7 resin is resistant to matrix damage that would reduce the stress concentration near the corners of the penetrator. Note that the ultrasonic methods used for the current study are unable to distinguish fiber failure zones.

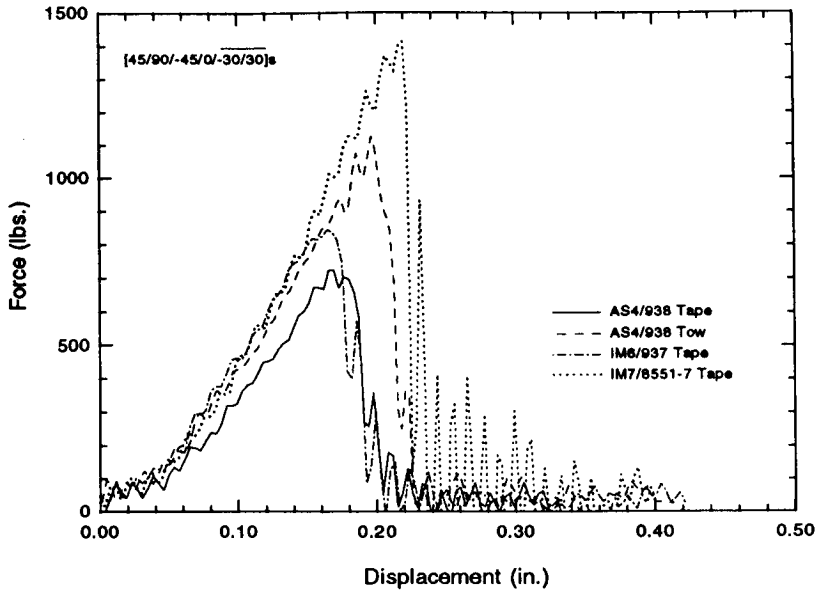

Figure 6: Instrumented Impact Results for Through-Penetration of AS4/938 Tow and Tape, IM6/3501-6, and IM7/8551-7

Force-displacement curves for tow-placed Crown1 laminates of 100% AS4/938, 100% S2/938, and Hybrid #3 (i.e., 50% AS4 / 50% S2 / 938, 12 tow repeat unit width) are presented in Figure 7. As expected from the fiber stiffness difference, the slope of the 100% S2/938 curve is less than that of the 100% AS4/938, and that of Hybrid #3 falls midway between. The total event energy of the S2/938 was over twice as large as that of the AS4/938, and the Hybrid #3 energy was midway between. Another conspicuous feature of the Hybrid #3 curve is the relative ductility of the failure, as compared to either the AS4/938 or S2/938.

Tension fracture strengths for specimens with 0.875 in. through-penetrations were compared to specimens with 0.875 in. machined cracks. The results are shown in Figure 8. In most cases, penetration strengths were within 10% of the machined-crack strengths, with the latter being higher.

The single configuration for which the penetration strength is more than 10% below the machined-crack strength is the IM7/8551-7 Crown1 laminate. The toughness of 8551-7 resin could conceivably create crack-tip extension significantly greater than that of the 937A and 938 materials, as alluded to in the discussion of instrumented impact results. An effective crack extension of approximately 0.25 in. on each side of the penetrator would result in a fracture strength that follows the trends of the machined cracks for IM7/8551-7. Future work involving deply of through-penetrated specimens will help to quantify fiber damage caused by the impact event.

The two configurations which have penetration strengths that are more than 10% higher than machined-crack strengths are the IM6/937A and AS4/938 Tape Crown2 laminates. The relatively high bending stiffness of the 16-ply Crown2 laminate may result in the formation of larger matrix splits and delaminations near the crack tip, thereby reducing the stress concentration and increasing the strength. Ultrasonic scans (e.g., Figure 9) confirmed the existence of larger delaminations in the Crown2 specimens.

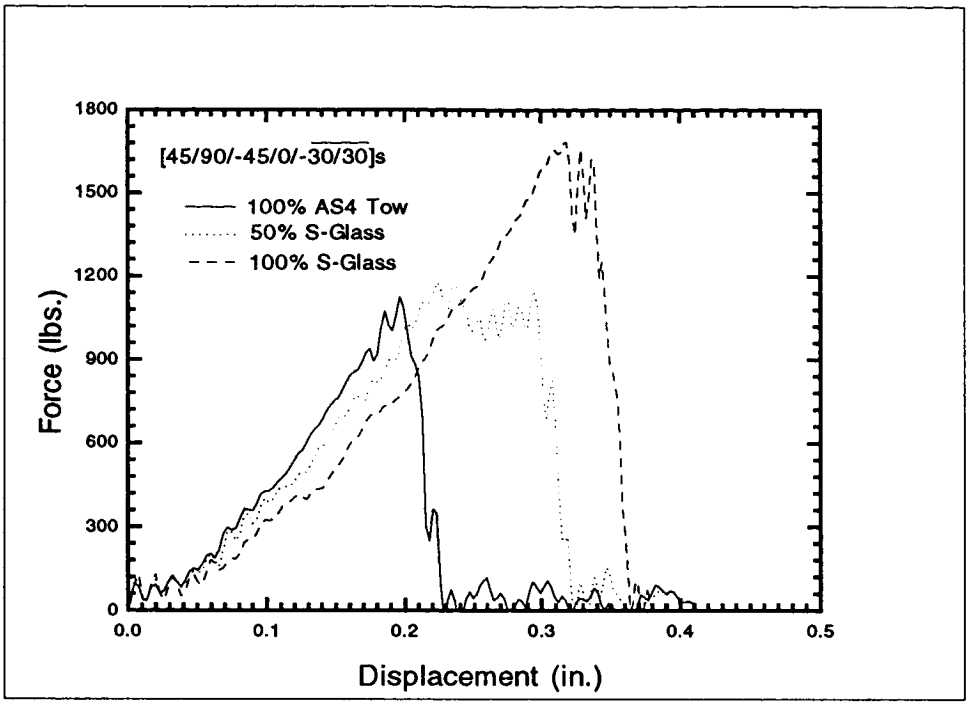

Figure 7: Instrumented Impact Results for Through-Penetration of Tow-Placed Laminates Consisting of Various Percentages of AS4 and S2

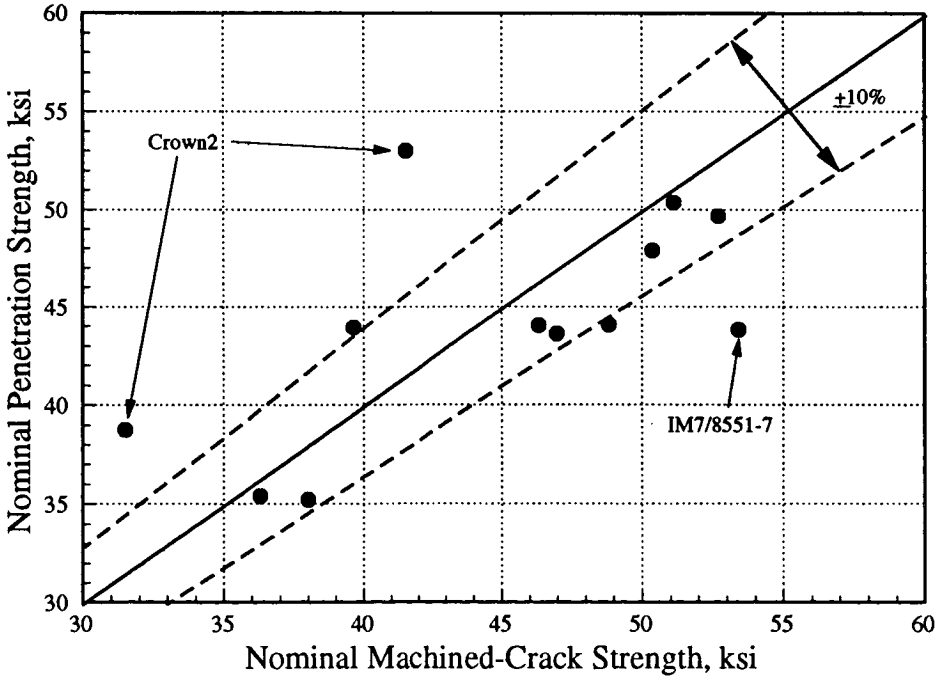

Figure 8: Comparison of Penetration and Machined-Crack Strengths

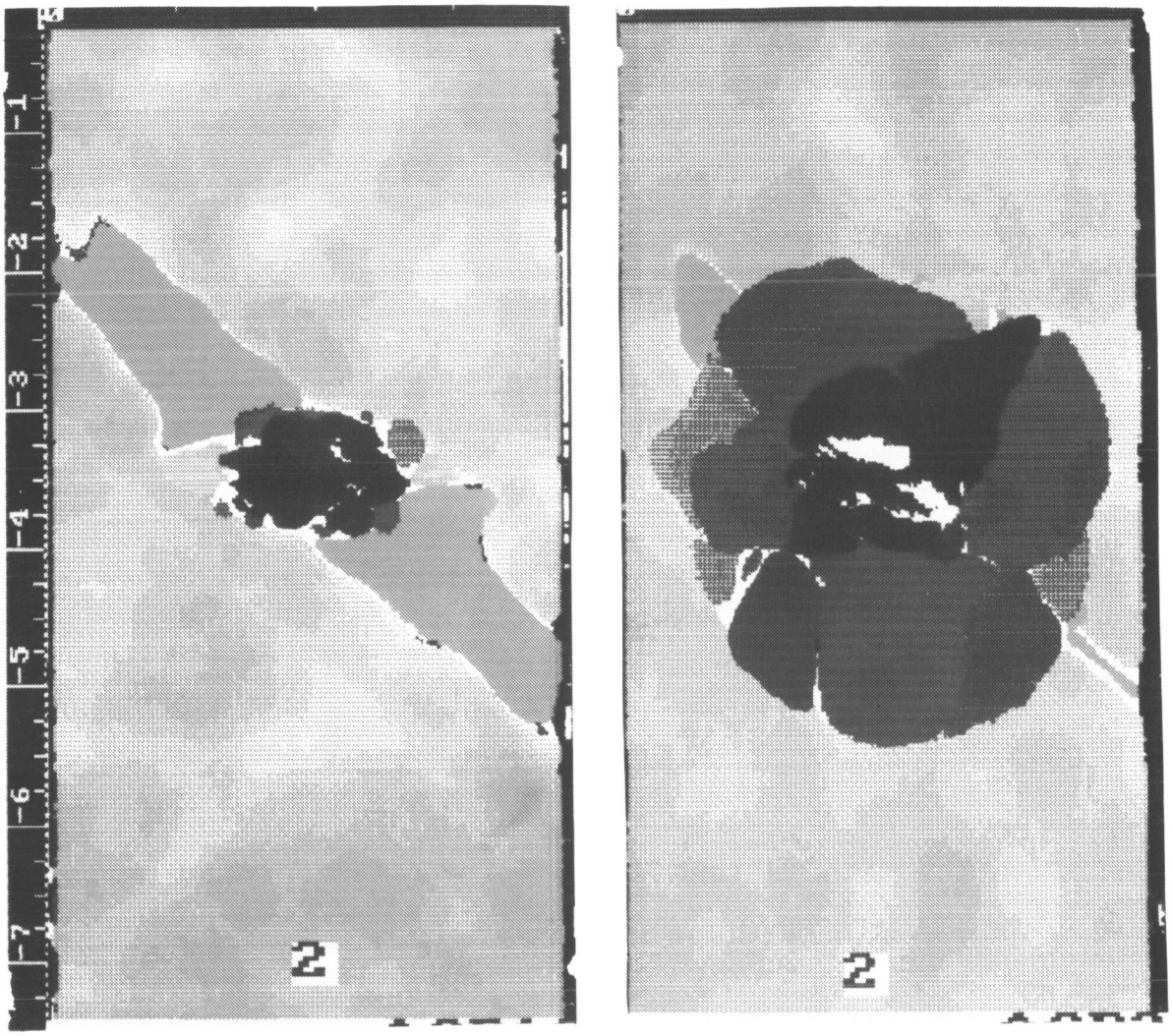

Crown1 Crown2

Figure 9: Ultrasonic C-Scans of AS4/938 Tape Crown1 and Crown2 Through-Penetration Specimens

Fiber Type

A representative comparison of the tension fracture strength of IM6/937A and AS4/938 tape systems for the Crown1 laminate is contained in Figure 10. For this layup and range of crack sizes, notched strength is higher for IM6/937A than AS4/938. A similar increase was seen for other layups. The IM6 fiber provides a 20 to 25% increase over AS4 in both fiber and unidirectional ply strengths. Since the laminate notched-strength of IM6/937A ranged from 5 to 25% greater than AS4/938, the fiber strength improvement of IM6 was not realized in all cases. Although IM6 appears to have some advantage in tension fracture performance over AS4, even a 25% improvement does not result in a crown design that is more economically attractive than an AS4 design (Ref. 2).

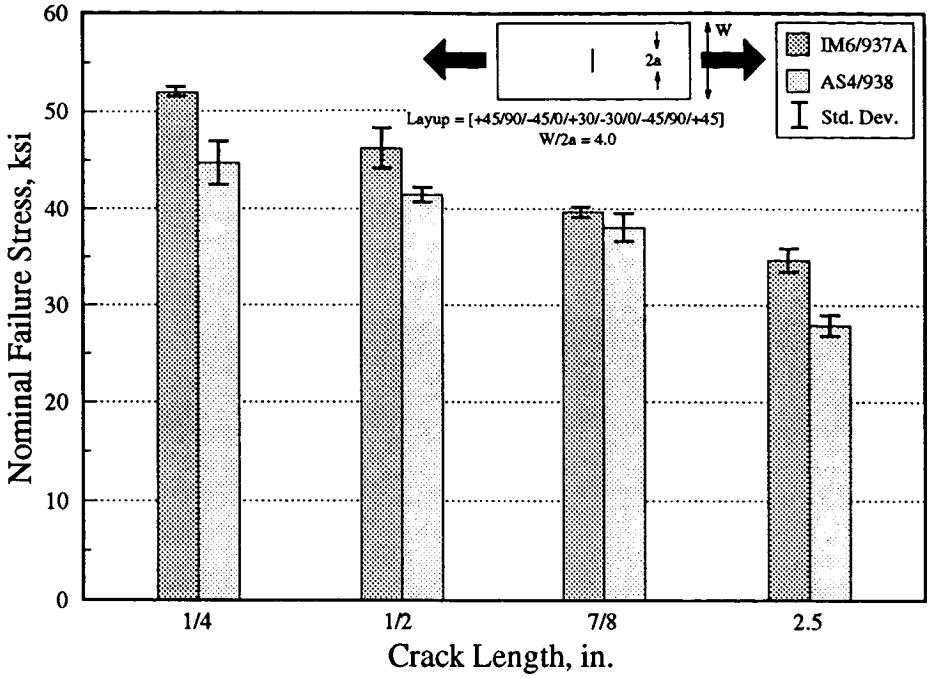

Figure 10: Comparison of Fracture Strength for IM6/937A and AS4/938 Tape

Resin Type

The effect of resin type was evaluated by comparing the fracture performance of IM7/8551-7 and IM6/937A tapes. Since IM6 and IM7 fibers are essentially identical, the behavior differences shown in Figure 11 are expected to relate to the resin type and how it bonds to the fiber. The IM7/8551-7 material exhibited approximately 35% greater strength for crack sizes less than 1 inch, but with a 2.5 in. crack, its strength was 7% below that of the IM6/937A. Similar findings were reported in Reference 14 between other brittle and tough resin systems.

Data for the 2.5 in. cracks supports a hypothesis that splitting in plies oriented along the loading direction enhances tension fracture performance of laminates having larger crack sizes. A Drexel University subcontract[13], supporting the ATCAS program, has studied the formation and growth of matrix splits in unidirectional specimens. The Drexel analysis and tests indicate that IM7/8551-7 is more resistant to matrix splitting than graphite fiber composites with matrices similar to 937A. The IM7/8551-7 material was also found to have G_{Ic} and G_{IIc} values for matrix damage growth that are 3 to 4 times as high as those of composites having the 937A-class resin. Despite the improved G_{Ic}, tests for mode I matrix cracking in IM7/8551-7 (Ref. 15) indicated that resin rich interlaminar layers reduce the "insitu strengthening effect" characteristic of multidirectional laminates.

---

[13] Ghaffari, S., Awerbuch, J., and Wang, A. S. D., "Temperature and Fracture Toughness Effects On Mixed Mode Matrix Splitting," Presented at the Fourth ASTM Symposium On Composite Materials: Fatigue and Fracture, 1991.

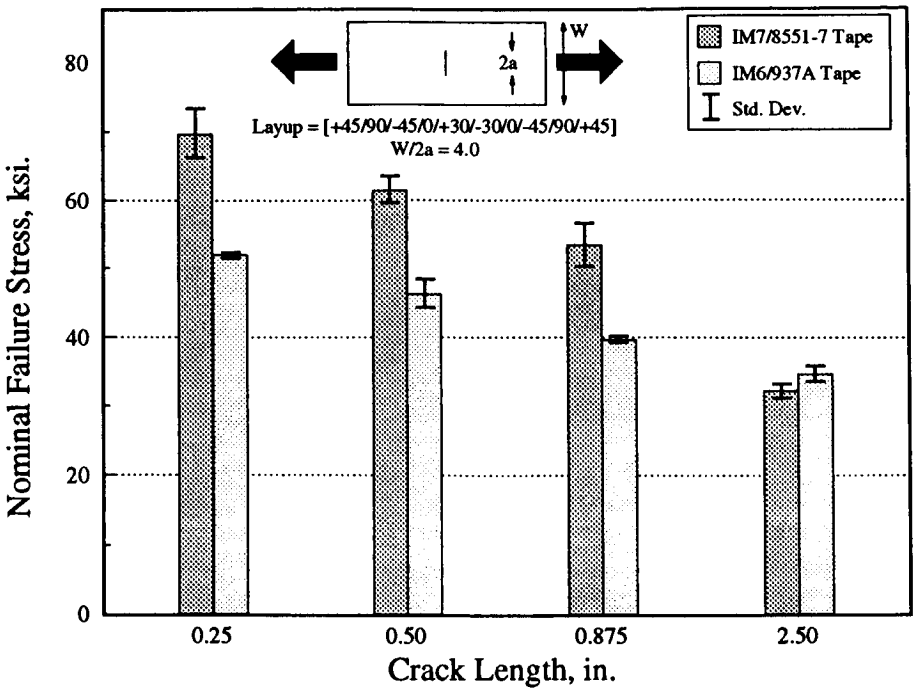

Figure 11: Comparison of Fracture Strength for IM7/8551-7 and IM6/937A Tape

Wang (Ref. 16) has shown that the initiation of matrix splitting in notched cross-ply laminates includes both mode I and II components of strain energy release rate, while subsequent stable growth is dominated by mode II. Conceivably, matrix splits will still form near cracks in IM7/8551-7 multidirectional laminates. However, mode II dominated split growth is resisted, leading to only minimal reduction of the stress concentration for larger cracks, and correspondingly lower tensile fracture strength. Additional discussions on this subject appear later in this paper.

Tow Material Form

Unexpected tension fracture results were found in comparing tow-placed AS4/938 laminates with similar tape laminates. As shown for machined cracks in Figure 12, the tow material was found to have a reduced sensitivity to crack length, with fracture strength improvements of approximately 10% for crack lengths below 1 in. and 25% for 2.5 in. cracks. This could be related to an enhanced mechanism of splitting parallel to the loading axis. Photomicrographs of cross-sections showed significantly higher amounts of intraply resin-rich zones in tow-placed laminates. These zones can serve as split-initiation sites. Other differences between tow and tape material forms which may have affected tension fracture include fiber sizing (tow fibers were sized, tape fibers were unsized), fiber bundle size (tow was 6K, tape was 12K), and resin impregnation method (tow was hot melt, and tape was solvent). Discussions in the analysis section of this paper will also hypothesize that tow-placed material forms have a higher dimensional level of inhomogeneity, tending to reduce the stress concentration for a range of crack sizes.

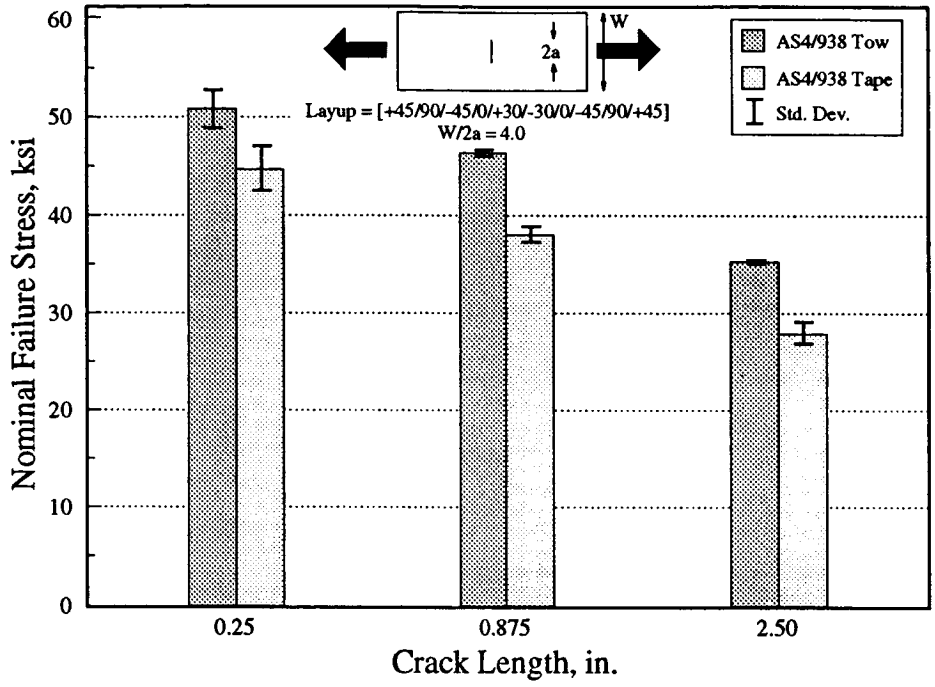

Figure 12: Comparison of Tension Fracture Strength of AS4/938 Tow and Tape

Intraply Hybridization

Results for the 8-run intraply hybrid designed experiment were analyzed (Ref. 17) using the factor levels shown in Table 1. Nominal failure stress and nominal failure strain (i.e., nominal failure stress/calculated modulus) were evaluated separately as response variables. Both measurements were corrected for finite width effects prior to data analysis. The finite width corrections were 7.6% and 3.8% for holes and cracks, respectively.

	Factor Level	
Factors	**Low (-1)**	**High (+1)**
(A) Hybrid Repeat Unit Width	0.38 in.	1.10 in.
(B) Percent S2-Glass (% by volume)	25%	50%
(C) Notch Type	Crack	Hole
(D) Notch Size	0.250 in.	0.875 in.

Table 1: Factor Levels for Intraply Hybrid Designed Experiment

The nominal values of failure stress and strain were found to have differing relationships with factors from the designed experiment. The following equations were generated based on regression analysis of experimental results:

Failure Stress, σ_{cr}, (ksi)

$$\sigma_{cr} = 49.90 - 0.83A - 1.74C - 2.86D - 0.92(AB \text{ or } CD)$$

Failure Strain, ε_{cr}, (% in./in.)

$$\varepsilon_{cr} = 0.785 - 0.014A + 0.057B - 0.028C - 0.045D - 0.016(AB \text{ or } CD) - 0.014(AD \text{ or } BC)$$

where the values for A, B, C, and D are taken as +1 or -1 (see Table 1). Only those regression terms affecting results by 3% or greater were included in the above equations. Both failure stress and strain were found to depend on notch size and notch type. Percent S2-Glass was found to have the strongest effect on failure strain, while having little impact on failure stress. The hybrid repeat unit width and possible two-way interactions were found to have small effects.

Experimental values of σ_{cr} and ε_{cr} were found to decrease on the order of 10% with increasing notch size (from 0.25 in. to 0.875 in.). The magnitude of residual strength decrease over this range of notch sizes was much less than that of traditional tape material forms (Ref. 3). For example, current results for AS4/938 and IM6/937A tape materials with the same layup (i.e., see Crown1 results in Figure 4) indicate strength reductions on the order of 15 and 25%, respectively. The reduced notch sensitivity of hybrid materials is similar to that observed for the AS4/938 tow-placed material.

Other hybrid variables found to have a significant effect on tensile fracture performance include notch type and percent S2-glass. Both σ_{cr} and ε_{cr} were found to be on the order of 7% lower for the specimens with holes than for those with cracks. Based on classical fracture theories, the opposite trend is expected for larger diameter holes and cracks. Future ATCAS tests will address this. The value of ε_{cr} tended to increase with increasing percent S2-glass, while σ_{cr} remained constant. This suggests that the increased ε_{cr} resulting from hybridization of AS4 (i.e., relatively low strain/high modulus fiber component) and S2-glass (i.e., relatively high strain/low modulus fiber component) was enough to counteract the drop in laminate modulus. Note that the hybrid designed experiment yielded results for relatively small notches. The ensuing paragraphs will discuss fully-crossed experimental results that show both σ_{cr} and ε_{cr} increase with percent S2-glass for a 2.5 in. crack.

The notched strengths of the hybrid materials were found to segregate from those of the tow-placed 100% AS4/938 material as notch size increased. For the AS4/S2 hybrids, the maximum increase in σ_{cr} was approximately 5% for both 0.25 and 0.875 in. notches; however, as illustrated in Figure 13, significantly larger increases (i.e., up to 17%) were seen at the 2.50 in. crack size. This trend may relate to interactions between percent S2-glass, hybrid repeat unit width, and notch size. The hybrid designed experiment results for relatively small notch sizes (i.e., 0.25 and 0.875 in.) indicated some interactions for the range of repeat unit widths analyzed.

Fracture tests for the fifth tow-placed hybrid, 75% AS4/25% T1000, were not part of the designed experiment. The T1000 fiber for this all-graphite hybrid has both a higher modulus and failure strain than AS4 fiber. A relative comparison of small notch results for the graphite hybrid and the tow-placed laminate consisting of 100% AS4 indicated an increase in σ_{cr} on the order of 10% for the former. Relative improvements in σ_{cr} for the 2.5 in. crack sizes were even higher (17% as shown in Figure 13). Considering the Crown1 layup used in fracture testing, axial modulus of the graphite hybrid was calculated to be 4.6% higher than that for a laminate with only AS4 fiber. By definition,

this resulted in a greater increase in σ_{cr} than in ε_{cr} when comparing the all-graphite hybrid and non-hybrid laminates. As was the case for tow-placed AS4/S2 hybrids, greater improvements for large notch sizes suggest possible interactions between hybridization parameters (e.g., percent T1000, hybrid repeat unit width) and notch size.

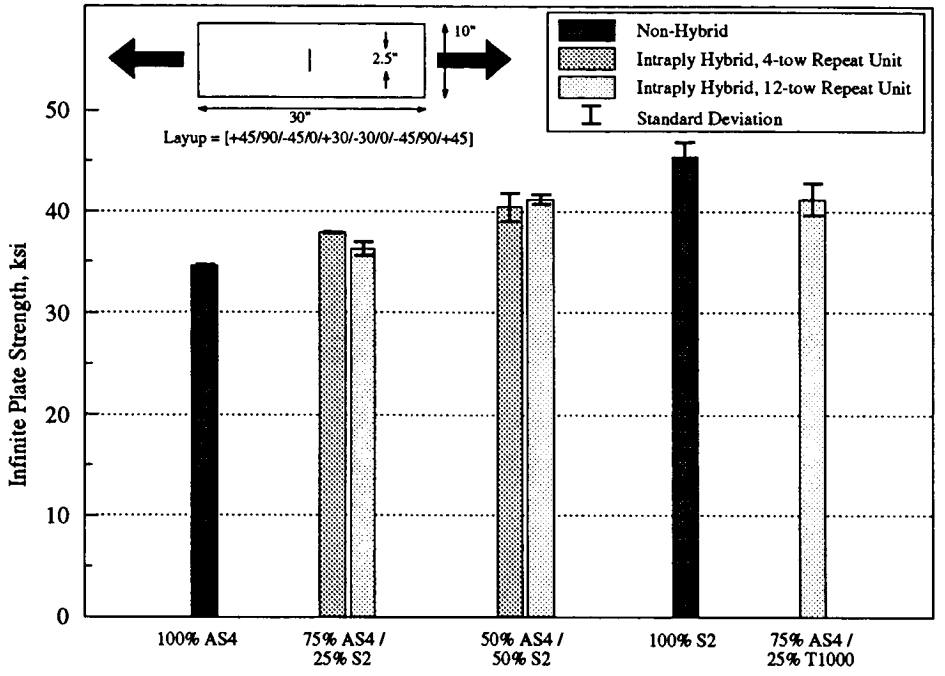

Figure 13: Tension Fracture Strength of Intraply Hybrids for 2.5 Inch Crack

Significant differences in failure were observed between the graphite tow-placed materials (i.e., 100% AS4 and Hybrid 5) and those containing any S2-glass (i.e., 100% S2-glass and Hybrids 1 through 4). The graphite specimens qualitatively appeared to exhibit relatively small amounts of crack-tip damage growth, while specimens with S2-glass exhibited large areas of matrix splitting and delamination prior to failure. As shown in Figure 14, the greater extent of crack-tip damage growth in S2-glass hybrids was confirmed by ultrasonic scans of failed 10 in. wide specimens with 2.5 in. initial crack length and a Crown1 layup. Note that higher failure strains correspond to greater damage levels for each of the four materials in Figure 14.

Another difference between graphite tow-placed materials and those containing any S2-glass relates to the load carrying capability of specimens after exceeding the maximum load. The all-graphite specimens exhibited brittle failures while those containing S2-glass continued to carry significant loads (often 30 to 40% of the peak load) after "failure." Evidence of this can be seen in Figure 15, which shows a failed 10 in. wide Hybrid #3 specimen with a 2.5 in. initial crack length and a Crown1 layup. The majority of the S2-glass fibers did not break, and, after failure of the graphite, rotated into the loading direction. Although the observed behavior for S2-glass hybrids depends on the use of displacement controlled tests, additional load carrying capability may better enable fuselage structures to sustain "get-home" loads following a discrete source damage event.

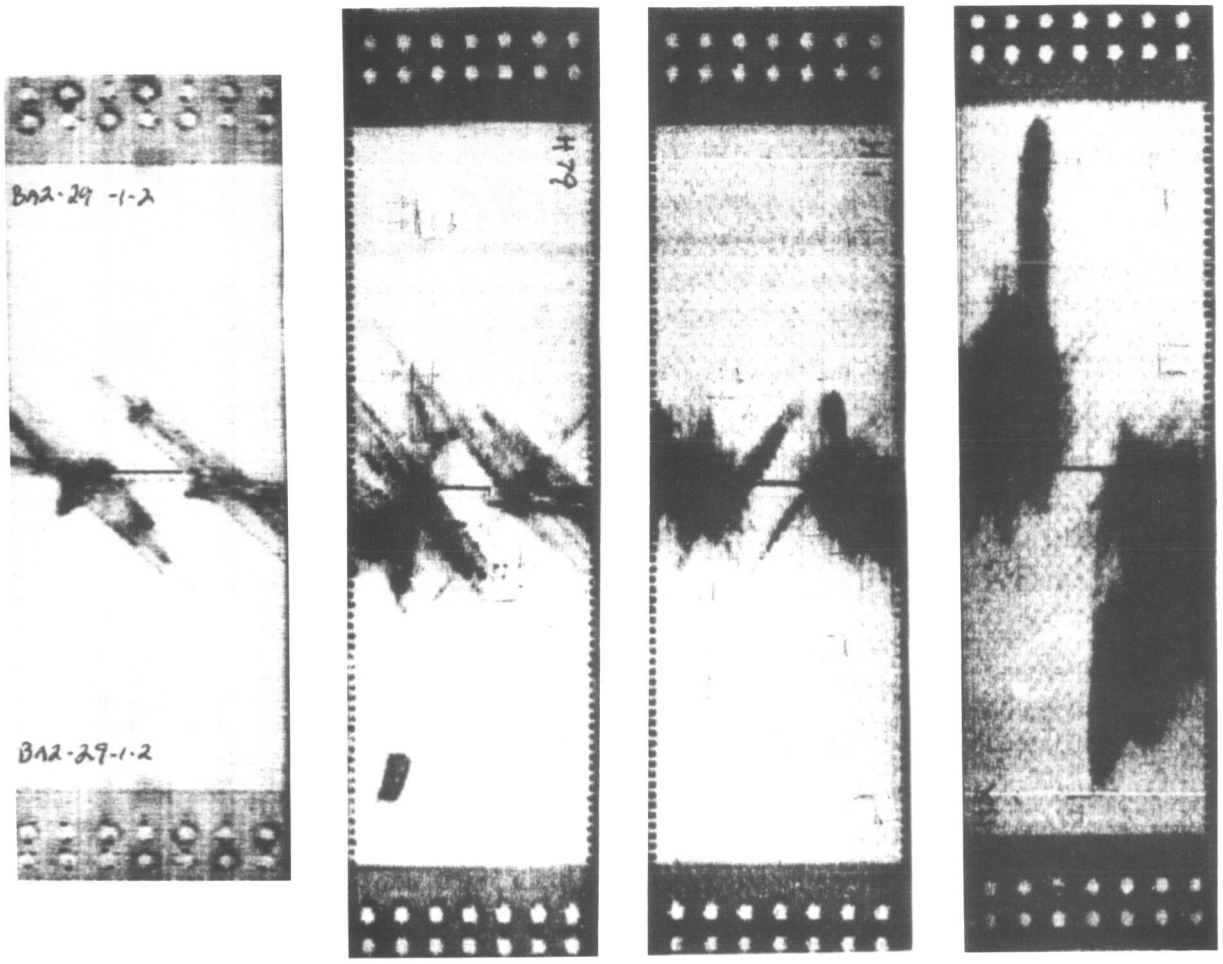

AS4/938 Tape	AS4/938 Tow	Hybrid #1	Hybrid #2
$P_{cr}/AE_x = .0039$	$P_{cr}/AE_x = .0050$	$P_{cr}/AE_x = .0059$	$P_{cr}/AE_x = .0075$

Figure 14: Ultrasonic Scans of Failed Fracture Specimens

Comparisons of Notch Sensitivity

For purposes of comparison in the current paper, notch sensitivity is defined as a change in fracture strength with increasing crack length. Figure 16 shows notch sensitivity data trends for six different material types. All data in the figure corresponds to averages for machined cracks, $W/2a = 4$, and the Crown1 layup. The six materials in Figure 16 are shown to have large differences in notch sensitivity. For the range of cracks tested (0.25 in. to 2.5 in.), IM7/8551-7 appears to have the greatest notch sensitivity (total drop of 54%), while Hybrid #3 had the least (total drop of 18%).

Data trends in Figure 16 also suggest that there is little correlation between fracture results for the smallest and largest cracks tested. For example, IM7/8551-7 had distinctly higher fracture strength than all other materials for a 0.25 in. crack, but had close to the lowest strength for a 2.5 in. crack. A series of statistical analyses was performed with the complete data set for Crown1 layups to confirm

this observation. Figure 17 shows results from regression analysis comparing 0.25 in. and 2.5 in. crack data for eight of the ten material types (due to the nature of a designed experiment two hybrids did not have test data for a 0.25 in. machined crack). This figure indicates that there is no correlation between data obtained at the two crack sizes.

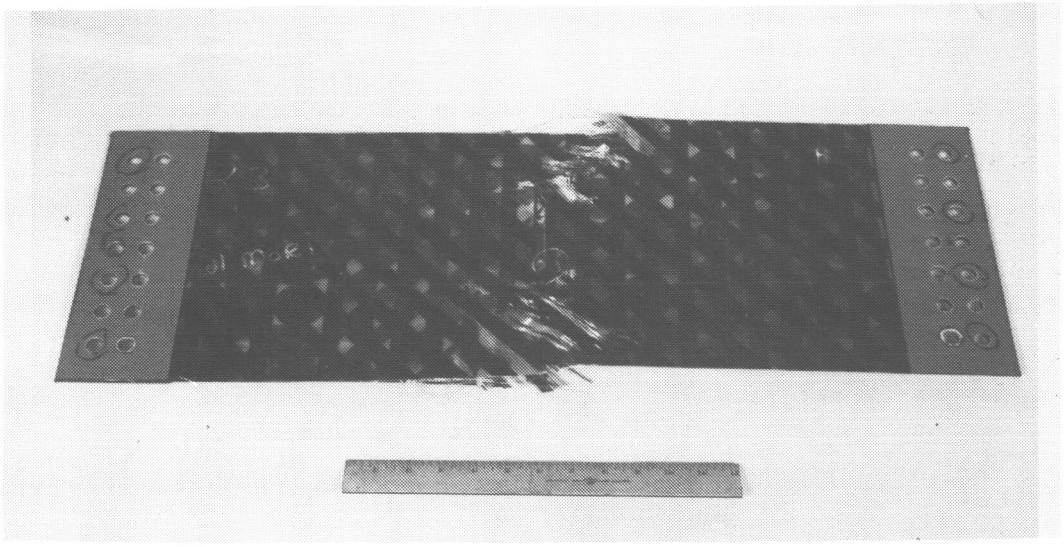

Figure 15: Failed Intraply Hybrid Tension Fracture Specimen

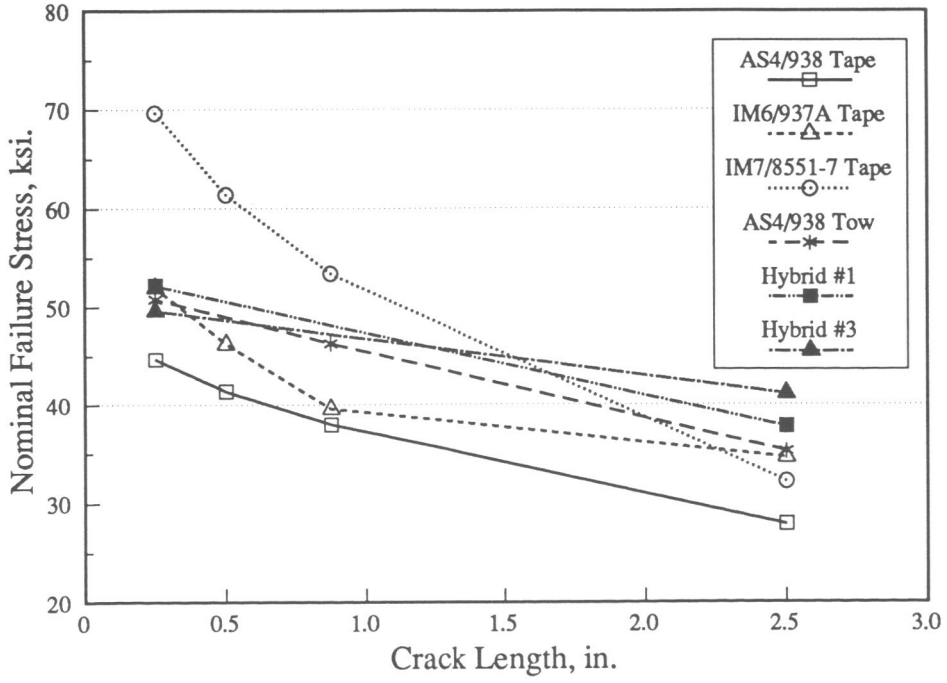

Figure 16: Comparison of Notch Sensitivity for Different Materials

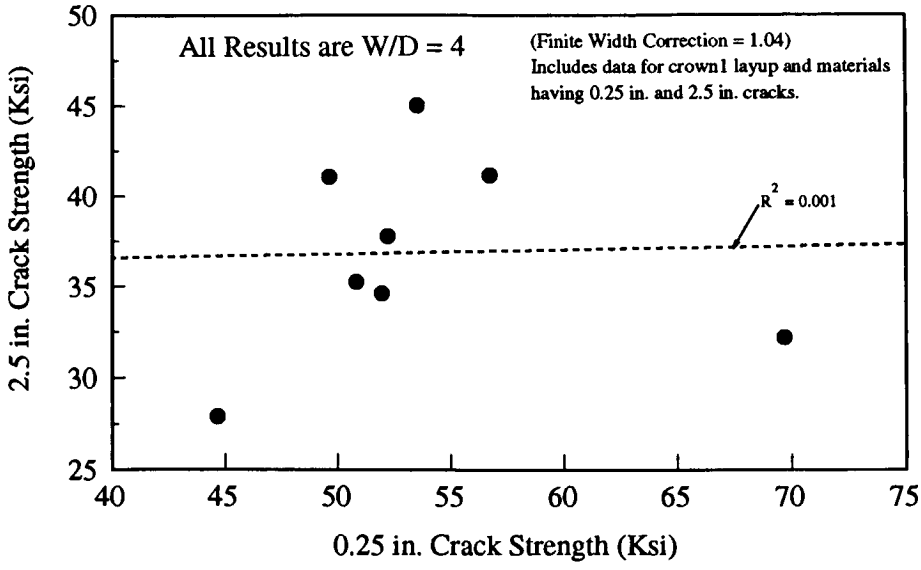

Figure 17: Statistical Relationship Between Small and Larger Crack Strengths

Results from other regression analyses indicated more favorable statistical correlations between fracture strengths at different crack sizes. A small correlation ($R^2 = 0.40$) was obtained between 0.875 in. and 2.5 in. crack test results. Better correlations ($R^2 = 0.78$) were obtained when comparing notched strength differences, e.g.,

$$(\sigma_{cr\{0.25\ in.\}} - \sigma_{cr\{2.5\ in.\}}) \text{ vs. } (\sigma_{cr\{0.25\ in.\}} - \sigma_{cr\{0.875\ in.\}}) \text{ and}$$

$$(\sigma_{cr\{2.5\ in.\}}/\sigma_{cr\{0.25\ in.\}}) \text{ vs. } (\sigma_{cr\{0.25\ in.\}} - \sigma_{cr\{0.875\ in.\}}) .$$

As mentioned earlier, an open hole specimen with a 0.25 in. diameter hole is commonly used in the aerospace industry to screen materials for notched tensile strength. Since holes and cracks are nearly equivalent for small notch sizes, results in Figures 16 and 17 suggest that the 0.25 in. notch test should not be used to screen materials for fuselage damage tolerance. An alternative procedure, involving a range of notch lengths is recommended later in this paper.

ANALYTICAL COMPARISONS

The primary purpose of tension fracture analysis methods is to provide failure predictions beyond the notch sizes and structural geometries tested during material characterization. To ensure this extrapolation capability, suitable models must revolve around theories with a basis in the physics of the problem. It is also desirable to minimize the number of degrees-of-freedom in a model to reduce material testing requirements. The following is a discussion of previously proposed analysis methods, and an evaluation of how well they predict the test data obtained in this program. Discussions of test data will be limited to the center-crack results, since the range of open-hole configurations was insufficient to evaluate predicted trends.

Finite Width Corrections

Correcting failure strengths for finite width effects provides the basis for comparison of different specimen configurations. Numerical methods have been employed to show that isotropic finite width correction factors (FWCF) differ from their orthotropic counterparts by less than 3% for specimen-width-to-crack-length ratios (*W/2a*) greater than 2 [Refs. 3, 18]. Any of the several expressions for isotropic FWCFs may therefore be used.

The current crack test database was used to assess the validity of using isotropic FWCFs. Nominal notched strengths, corrected for finite width according to

$$\sigma_N^{\infty} = FWCF * \sigma_N, \qquad (1)$$

where $FWCF = 1 + 0.1282\,(2a/W) - 0.2881\,(2a/W)^2 + 1.5254\,(2a/W)^3$,

were compared for all laminates fabricated from both AS4/938 and IM6/937A tape. Test data were plotted as finite-width-corrected strength versus crack length for each of $W/2a = 4$ and $W/2a = 2$, as shown in Figure 18 for the AS4/938 Crown1 laminate. Properly corrected data should fall on a single curve. For every laminate, however, the $W/2a = 2$ data was lower than that of $W/2a = 4$. This difference was quantified by comparing average strengths for equivalent crack lengths, and found to be between 4 and 30% of the $W/2a = 4$ values.

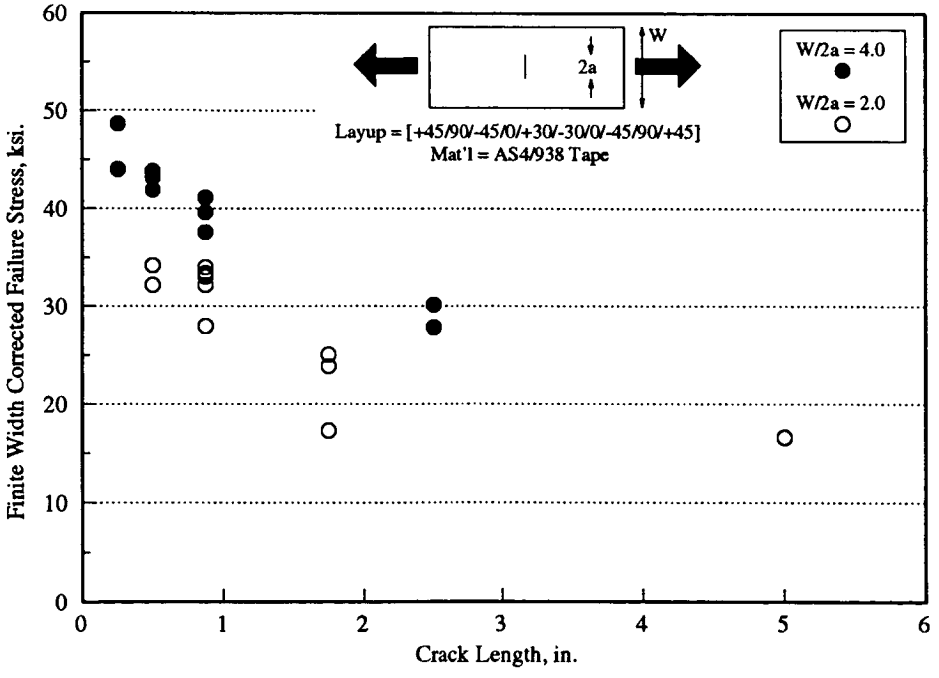

Figure 18: Comparison of Finite Width Corrected Strengths for *W/2a* = 2 and *W/2a* = 4

Experimental results clearly indicate that FWCFs for $W/2a = 2$ data are consistently underpredicted. Several phenomena not considered in the development of the FWCF relationships may account for this shortcoming. These are: (a) specimen edge-delamination, (b) crack-tip softening due to matrix damage, and (c) buckling adjacent to the unsupported crack surfaces due to Poisson's-ratio-induced transverse compression.

Specimen edge delamination and crack-tip matrix damage act to increase the stress-field interaction with the boundary. Edge delamination causes an in-plane stiffness reduction in the vicinity of the delamination, resulting in load redistribution toward the center of the specimen. Similarly, crack-tip matrix damage reduces the stiffness near the crack tip, resulting in load redistribution towards the edge of the specimen. Both of these phenomena were observed to varying extents during the tests. The increased interaction with the boundary is more pronounced in lower *W/2a* specimens, since a higher percentage of the net area is affected. A larger increase in the actual FWCF for *W/2a* = 2 specimens therefore results.

Transverse buckling adjacent to the unsupported crack surface was observed in both the 2.5 in. and 5.0 in. crack specimens, and was confirmed with the measurement of out-of-plane displacements of up to several times the specimen thickness at 75 to 80% of the failure load. The transverse buckling reduces in-plane stiffness in a somewhat circular region, resulting in behavior resembling that of a partially-filled hole. The FWCF for the crack with transverse buckling, therefore, increases towards that of a hole. As shown in Figure 19, the FWCF difference between a crack and a hole (Ref. 19) is much larger for *W/2a* = 2 than for *W/2a* = 4.

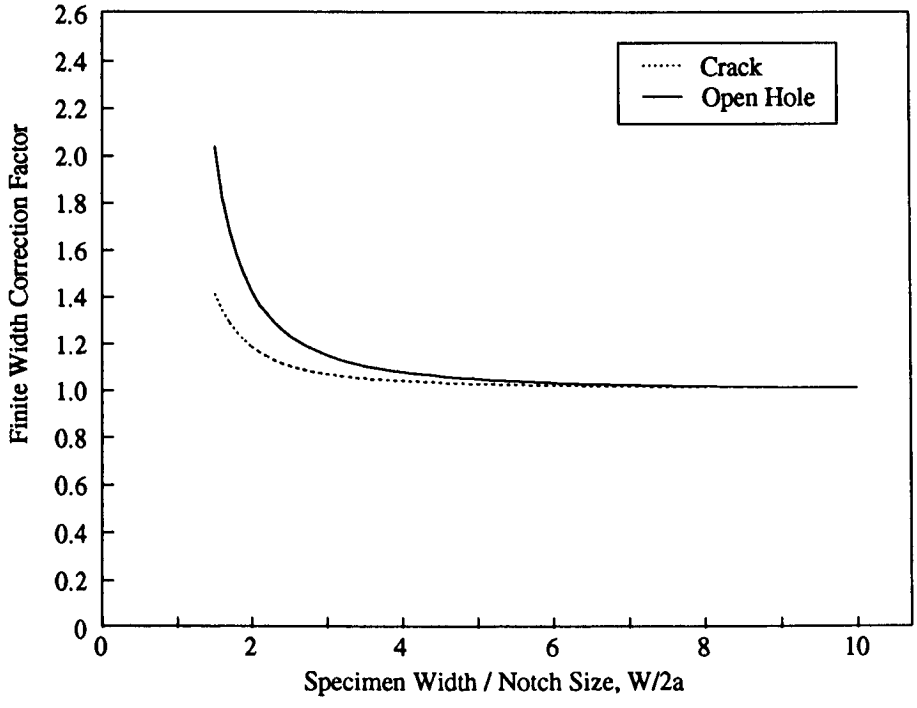

Figure 19: Comparison of Finite Width Correction Factors for Cracks and Open Holes

Due to the uncertainty in correcting test data with differing *W/2a* values, the remainder of the comparisons with test data in this paper are limited to those data with *W/2a* = 4. Many of the studies in the literature (as reviewed by Ref. 3) increased crack length for a constant width specimen, with the largest cracks typically being tested in the *W/2a* = 2 range. This results in the residual strength curve being errantly skewed downward at the larger crack lengths. Limiting comparisons to *W/2a* = 4 reduces this problem.

Review of Failure Criteria

Several failure criteria that have been proposed for tension fracture were evaluated. In the following discussion of the criteria, σ_N^∞ and σ_o are the notched and unnotched strengths of an infinite plate, respectively, and a is the half-crack length.

The stress distribution at a crack tip is singular for classical continuum theories. In linear elastic fracture mechanics (LEFM) for homogeneous materials, a square-root singularity exists, and failure is predicted by

$$\sigma_N^\infty = K_{Ic}/(\pi a)^{1/2} \tag{2}$$

where K_{Ic} is the critical stress intensity factor. This approach suffers from the physically unacceptable situation of infinite stresses at the crack tip. As a consequence, σ_N^∞ increases rapidly with decreasing a and σ_o becomes infinite, in the limit, as a approaches 0.

In composites, this has been addressed by several theories through the use of a characteristic dimension, inherent flaw size or critical damage zone length. The Whitney-Nuismer (WN) point-stress criteria (Refs. 20, 21), for example, predicts failure when the stress at a characteristic dimension, d_1, ahead of the crack tip equals or exceeds σ_o. The notched strength, then, is given by

$$\sigma_N^\infty = (1 - (a/(a + d_1))^2)^{1/2} \tag{3}$$

The two parameters in this model which must be determined are σ_o and d_1.

The Pipes-Wetherhold-Gillespie (PWG) model (Refs. 22, 23) extends the WN point-stress model to include an exponential variation of d_1 with crack length. This provides added flexibility in predicting small crack data, but requires an additional parameter to be determined.

Another multi-parameter model, proposed by Tan (Ref. 24), uses a characteristic dimension to predict failure of a plate with an elliptical opening subjected to uniaxial loading. In this model, a high-aspect-ratio ellipse is used to simulate a crack. Notched strengths are predicted by factoring the actual unnotched laminate strength by the ratio of predicted notched to predicted unnotched strengths. Both of these predicted strengths are obtained using a quadratic failure criterion in conjunction with the first-ply-failure technique. The predicted notch strength is determined by applying the failure criterion at a characteristic dimension away from the crack. The coefficients in this criterion are the additional parameters that must be determined.

The Poe-Sova (PS) model (Refs. 25, 26) may also be formulated with a characteristic dimension, d_2, but predicts failure when the *strain* at that distance ahead of the crack tip equals or exceeds the fiber failure strain. The notched failure stress is given by

$$\sigma_N^\infty = \sigma_o/(1 + (a\xi^2/2d_2))^{1/2} \tag{4}$$

where ξ is a functional that depends on elastic constants and the orientation of the principal load carrying plies. The characteristic dimension relates to a material toughness parameter, which was found to be relatively independent of layup. The two parameters which must be determined for this model are the fiber failure strain and d_2.

Two other frequently-used models, Waddoups-Eisenmann-Kaminski (WEK) and WN average stress, each have undamaged strength as the first parameter. The second parameters for WEK and WN average stress models are referred to as critical damage size and average stress characteristic dimension, respectively. The WEK model (Ref. 27) applies LEFM to an effective crack that extends beyond the actual crack by the inherent flaw size. The WN average stress model (Refs. 20, 21)

assumes failure when the average stress across the characteristic dimension equals or exceeds σ_o. Both the WEK and WN average stress models were found to be functionally equivalent to the PS model if a linear strain-to-failure is assumed.

The approaches described above which use a length parameter (e.g., characteristic dimension) were formulated to account for observed experimental trends for composites. In practice, these length parameters are determined from notched strength data and given limited physical meaning in relationship to any microstructural dimension of the material. They are often thought of as classical analysis correction factors, which enable the user to account for apparent changes in the stress distribution or fracture toughness with increasing crack size. It should be noted that the length parameter calculated for the WN point stress, WN average stress, PS, WEK, and Tan models will generally take on different values for the same set of data.

A more physically acceptable approach to predicting composite fracture may involve changes in the crack tip stress distribution as a function of material length parameters that define levels of inhomogeneity. Simplified analysis performed to evaluate the effect of inhomogeneities at the fiber/matrix scale indicated that the crack size should be at least three orders of magnitude larger than the fiber diameter to vindicate the classical continuum homogeneity assumption (Ref. 28). The results of Reference 28 show that inhomogeneity tends to reduce stress intensity factors for a range of crack lengths that is related to the level of inhomogeneity. Considering the fiber/matrix dimensional scale, the crack length range affected by inhomogeneity is smaller than that for which characteristic lengths are needed to correct classical fracture analyses for graphite/epoxy composites. However, higher levels of inhomogeneity exist in tape and tow-placed laminates due to manufacturing processes. These characteristics of composite materials may be responsible for the reduced stress concentrations traditionally found for small cracks.

Solutions to fracture problems using generalized continuum theories have also yielded results consistent with experimental trends in composites, without a semi-empirical formulation. Generalized continuum theories are formulated to have additional degrees of freedom which characterize microstructural influence. The stress concentrations for such theories change as a function of relationships between notch geometry and material characteristic lengths (e.g., Refs. 29, 30, and 31). Note that the characteristic lengths of generalized continuum are different than those in models described earlier because they are fundamentally based on moduli from the theory. As a result, the moduli have relationships with other material behavior (e.g., wave propagation) and their values can be confirmed from a number of independent experimental measurements. Ultrasonic wave dispersion measurements have been used to predict the moduli and notched stress concentration for wood composite materials (Ref. 29). Unfortunately, considerably more work is needed to develop generalized continuum theories for applications with laminated composite plates.

For inhomogeneous materials, the stress distribution at the crack tip is also not limited to a square-root singularity. The Mar-Lin (ML) model (Refs. 32, 33) allows the singularity, n, to be other than square-root. The notched failure stress is given by

$$\sigma_N^{\infty} = H_c/(2a)^n \qquad (5)$$

where H_c is the composite fracture toughness. In general, H_c and the exponent n are the two parameters that must be determined. In the Reference 32 and 33 studies, the exponent, n, was related to the theoretical singularity of a crack in the matrix, with the tip at the fiber/matrix interface. For this case, the singularity is a function of the ratio of fiber and matrix shear moduli and Poisson's ratios. Using this method, the singularities for a range of typical fiber/matrix combinations were determined to be between 0.25 and 0.35.

The Tsai-Arocho (TA) model (Ref. 34) combines the non-square-root singularity of the ML model with the inherent flaw concept of the WEK method. At the expense of another parameter, additional flexibility in predicting small-crack strengths is gained, although this effect lessens as the order of the singularity is reduced.

Other theoretical approaches which have been applied to predict tension fracture in composites include damage zone models, DZM (e.g., Ref. 35 and 36), and progressive damage analysis, PDA (e.g., Ref. 37 and 38). Both methods use finite elements to account for notch tip stress redistribution as damage progresses. The DZM utilized a Dugdale/Barenblatt type analysis for cohesive stresses acting on the surface of an effective crack extension over the damage zone length. As was the case for characteristic-length-based failure criteria described above, a Barenblatt analysis (Ref. 39) resolves the stress singularity associated with cracks. The PDA methods account for the reduced stress concentration associated with mechanisms of damage growth at a notch tip by reducing local laminate stiffness. From a practical viewpoint, both DZM and PDA methods may be more suitable in calculating the finite width effects discussed in the previous subsection and for predicting the performance of final design concepts; however, applications of finite-element-based methods during design concept selection are limited.

Functionality of Criteria

This subsection will review the degrees of freedom in curves from two parameter models which have been used extensively to predict tension fracture for composite laminates. This background will help to interpret discussions that compare theory with the current experimental database in the following subsection. Predictions for both small crack ($2a \leq 1.2$ in.) and large crack ($2a$ up to 20 in.) sizes will be compared. The former crack sizes are characteristic of most data collected for composites to date. Four theories will be covered in detail; classical LEFM, WN (point stress), PS (point strain), and ML. As a baseline for comparing changes in crack length predicted by the four theories, curves will be generated based on average experimental results (finite width corrected) for the IM6/937A tape material with Crown1 layup and $W/2a = 4$. This will ensure that all theories agree for at least one crack length.

Figure 20 shows a comparison of the four theories for small crack sizes. Only a small difference is seen between PS and WN criteria. A close examination of the LEFM and ML curves indicates that the singularity has a significant effect on curve shape. For crack lengths less than the baseline point, ML predictions are less than those of LEFM. For crack lengths greater than the baseline point, the opposite is true, and theories tend to segregate based on singularity (i.e., WN, PS, and LEFM yield nearly the same predictions).

Figure 21 shows that singularity dramatically affects differences between predictions in the large crack length range. The ratio of notched strength predictions for theories with the same order of singularity becomes a constant. For example, WN and LEFM become functionally equivalent and the relationship:

$$K_{Ic} = \sigma_o (2\pi d_1)^{1/2} \qquad (6)$$

will yield a value for K_{Ic} such that the two theories compare exactly for large cracks.

In order to compare the effect of a range of singularities on notched strength predictions, curves in Figures 22 and 23 vary the value of n from 0.1 to 0.5. All curves in Figure 22 cross at the baseline point used to determine the corresponding fracture toughness values. By allowing both variations in fracture toughness and order of singularity, the ML criterion could statistically fit a wide range of notched strength data trends for small crack sizes. Such an approach is not recommended for other

than interpolation purposes, because Figure 23 clearly shows how projections to a large crack size is strongly dependent on the assumed singularity.

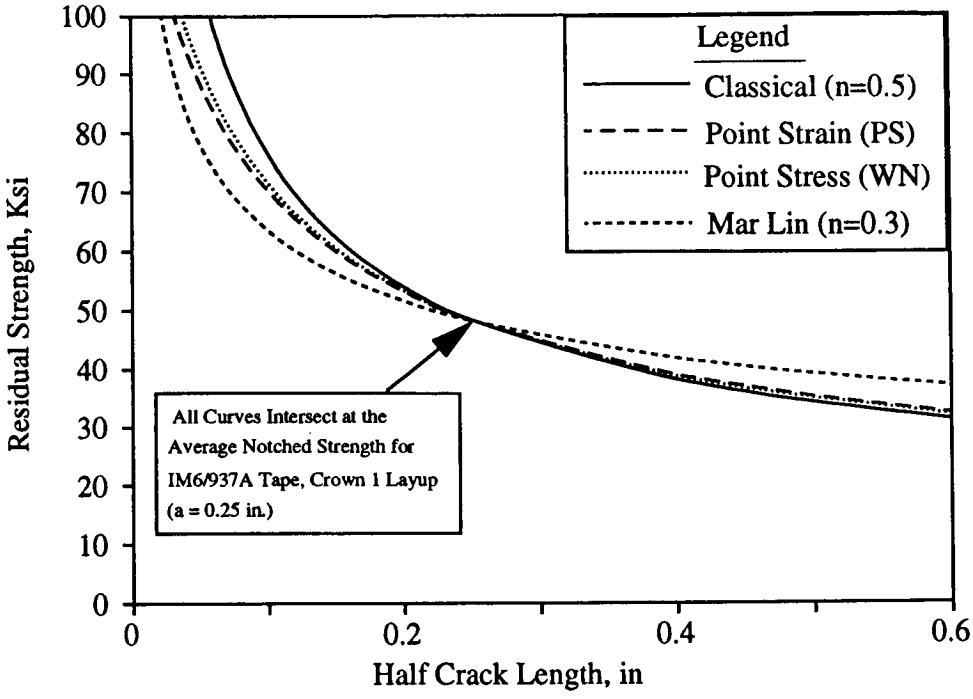

Figure 20: Comparison of Curve Shapes for Notched Strength Prediction Theories in Small Crack Range

Figures 24 and 25 show how the two parameters in the WN point stress criteria, σ_o and d_1, affect both the shape and relative positions of notched strength curves. Again comparisons are made with classical LEFM equations passing through common points. The lower set of curves corresponds to the baseline data point. Unlike the LEFM curves which rise sharply with decreasing crack length, the point stress theory has a finite strength, σ_o, at $a = 0$. For a given value of σ_o, increasing d_1 tends to increase the predicted notched strength and, hence, has an effect similar to increasing K_{Ic} in LEFM (see upper curves in Figures 24 and 25).

In the small crack length range, a reduced value of σ_o can have the appearance of reducing the singularity. The curve shapes for lower curves in Figure 24 indicate that various combinations of σ_o and d_1 could be selected to represent data trends that follow any of the singularities shown in Figure 22 (particularly for $a \leq 0.25$). For small crack sizes characteristic of past databases, the curve-fits for WN and ML theories are nearly indistinguishable (Ref. 3). This inability to distinguish lower orders of singularity in past composite data may relate to measured values of σ_o that were low due to edge delamination phenomena in finite width specimens. For large crack lengths, Figure 25 shows that the magnitude of σ_o and d_1 determine residual strength, but curve shape is dominated by the order of singularity. As discussed in reference to Figure 23, the proper order of singularity is best judged at large crack lengths.

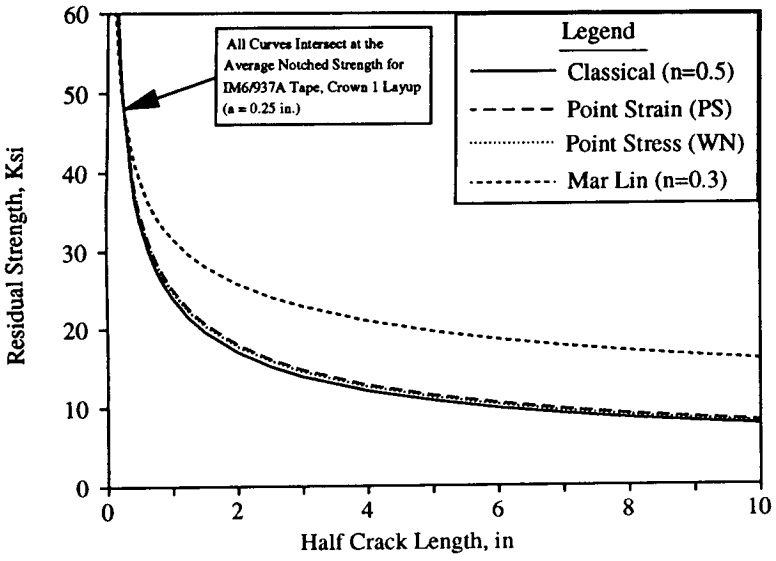

Figure 21: Comparison of Curve Shapes for Notched Strength Prediction Theories in Large Crack Range

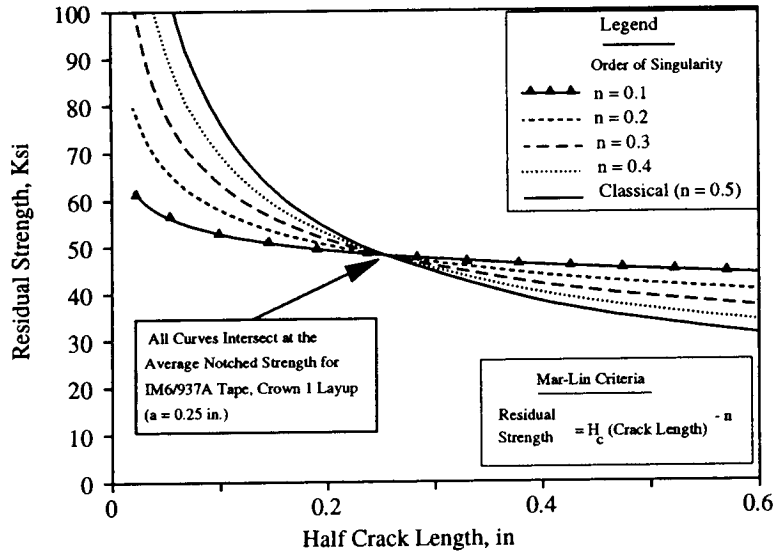

Figure 22: Effect of Singularity on Curve Shapes for Notch Strength Prediction Theories in Small Crack Range

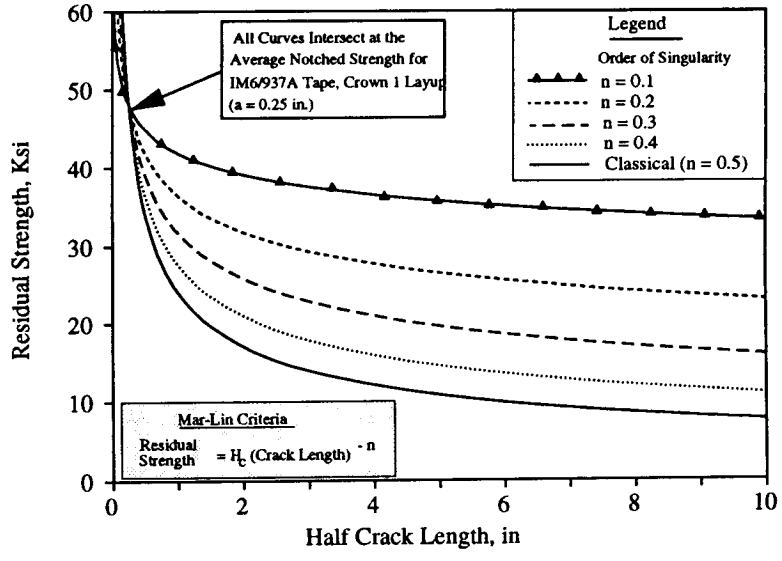

Figure 23: Effect of Singularity on Curve Shapes for Notch Strength Prediction Theories in Large Crack Range

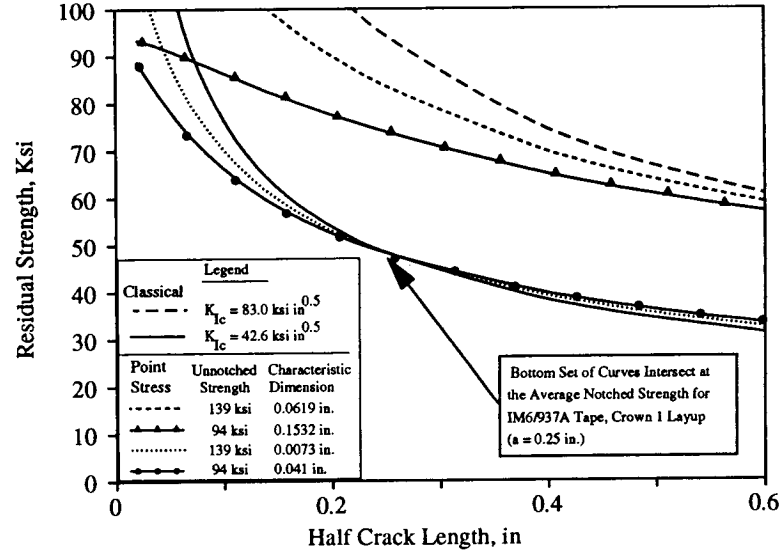

Figure 24: Effects of Characteristic Dimension and Unnotched Strength on Curve Shapes for Notch Strength Prediction Theories in Small Crack Range

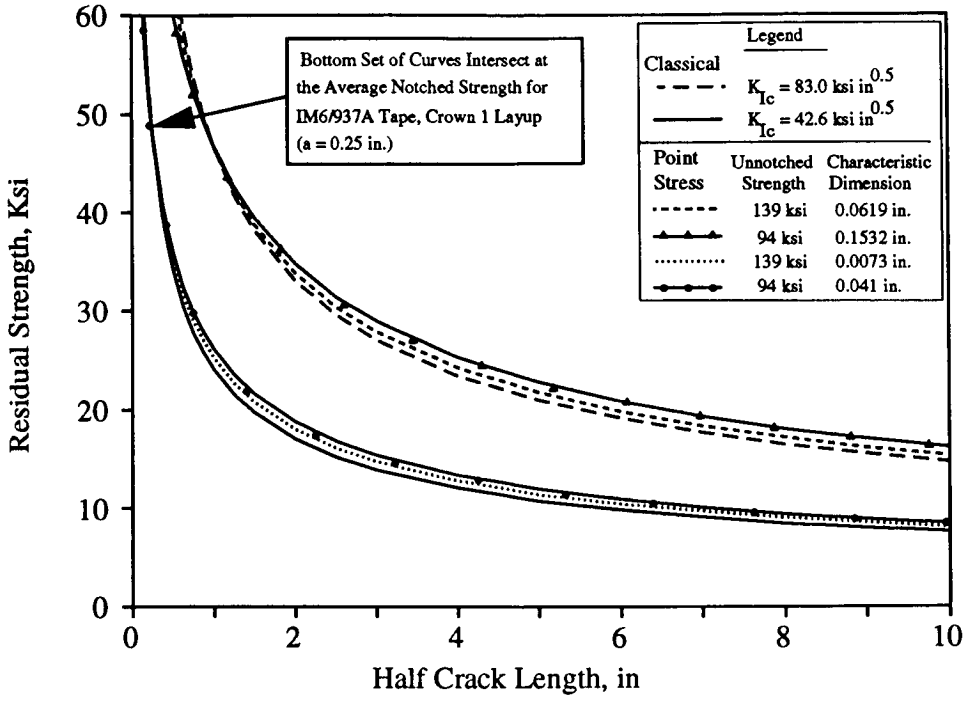

Figure 25: Effects of Characteristic Dimension and Unnotched Strength on Curve Shapes for Notch Strength Prediction Theories in Large Crack Range

Comparison With Test Results

Test data collected to screen materials for fuselage applications also provided a basis to evaluate the various failure criteria. Evaluations were made for laminates of practical interest to fuselage skin structures (i.e., multidirectional laminates having some percentage of both 0° and 90° plies). As in the application of fracture mechanics to metallic structures, suitable failure criteria use specimen data from material characterization tests to predict fracture of structural geometries. Structural variables are a subject of future ATCAS activities; however, the current study provides data to evaluate the theories for variable crack length.

Applications documented in the literature have advised using experimental data for a range of crack lengths to determine semi-empirical parameters in the composite notched failure criteria (e.g., Ref. 3). This may be achieved by using a least squares statistical curve fit with the proper function. Alternatively, the parameters can be determined for each crack length in the database and a scatter plot versus crack length can be used to judge if the parameter remains constant. This alternative approach was adopted for evaluating theories in the current study. Model parameters that were predetermined, independent of the notched fracture data, include the unnotched strength (σ_o) and order of singularity (n). Note that the order of singularity was set at 0.3 for the ML criteria. This reduced the number of parameters determined directly from notched test data to one for each of the four failure criteria evaluated in this section.

Due to the phenomena of edge delamination, finite specimen width is known to reduce the unnotched tensile strength measured for laminates. Tension test results from unnotched tubular specimens (Ref. 40) showed that quasi-isotropic laminates consisting of AS4/3501-6 tape materials (similar to AS4/938 used in current study) fail at a strain very close to the fiber failure strain measured in tests with

unidirectional specimens. To avoid finite width effects in determining the value of σ_o, it was calculated for laminates that had plies oriented in the axis of load by

$$\sigma_o = E_x \varepsilon_{cr}$$

where E_x was the laminate modulus in the direction of load (calculated based on lamination theory and measured lamina properties) and ε_{cr} was the measured axial fiber failure strain from unidirectional tests. In the case of hybrid materials, methods described by Chamis (Ref. 41) were used to calculate E_x. The hybrid ε_{cr} was assumed to be that of the fiber with the lowest value (i.e., unidirectional laminate test data for AS4/938 in all cases).

In an attempt to minimize the width effect discussed earlier, all failure criteria evaluations were performed using data for $W/2a = 4$. To determine parameters for the failure criteria, the average values printed in Figure 4 were corrected for finite width (FWCF = 1.04). Scatter plots of the fracture parameters versus crack length were generated for each multidirectional layup and material type. As expected, the classical fracture mechanics approach yielded an increasing K_{Ic} with increasing crack length for all cases. In most cases, the value of K_{Ic} doubled for crack lengths ranging from 0.25 in. to 2.5 in.

Composite failure theories evaluated in the current study were all found to have better correlation with experimental data than the classical K_{Ic} approach. However, values of composite fracture parameters (d_1, d_2, H_c) were also found to have significant increases with increasing crack length for most materials and layups studied. For example, values of H_c increased by up to 50% for crack lengths ranging from 0.25 in. to 2.5 in. The current authors recognize that these findings generally differ from those reported by Awerbuch and Madhukar (Ref. 3) in a review of fracture data available in the literature.

Significant differences in evaluations of the current database and those obtained in most past studies include:

1. The longest cracks considered in the current study were larger than those considered in most past studies.
2. Current analysis comparisons were made with variable crack length data obtained from specimens having a constant $W/2a$ (i.e., the FWCF was the same for all data).
3. Tension test values obtained for σ_o and used in failure criteria for past studies may have been low due to edge delamination in finite width specimens.

As illustrated in the previous subsection, a wide range of crack lengths is needed to distinguish differences in the various composite failure criteria. Results shown earlier in this paper indicated that classical FWCF for small $W/2a$ are inaccurate. This may have resulted in misleading trends in past studies that compared theory to variable crack length data obtained for constant specimen width (i.e., the FWCF used to facilitate the comparison changed with increasing crack length). As a result, the past studies may have overlooked the effects of the assumed singularity which is dominant for larger crack lengths. Finally, low values for σ_o can tend to mask possible limitations of theories applied to small crack data.

A close examination of the theories and experimental data for specific layups and material types revealed several interesting trends. For some materials and layups, specific fracture parameters became constant for the two largest cracks in a data set. In agreement with theory, the fracture strength for the largest crack sizes appeared to become dependent on the order of singularity and a constant value of fracture toughness. In the case of the thickest laminates tested (16 ply), some failure

parameters were constant for the full range of crack lengths. Several graphs will be used in the remainder of this subsection to illustrate the observed trends and discuss strengths and weaknesses generally found for the failure criteria evaluated.

Figure 26 shows results for the material with a toughened matrix, IM7/8551-7. The comparison between theory and experiment was made by using fracture parameters determined from the average strength data for the largest crack length. Results suggest that a singularity of 0.5 best represents data trends for large crack lengths. Out of all the materials and layups studied, this trait was found to be unique to the IM7/8551-7 material. Note that, of the square-root singularity methods, WN and PS best follow data trends for the smaller crack lengths, but values of d_1 and d_2 would need to increase with crack length for a good fit of the entire data range.

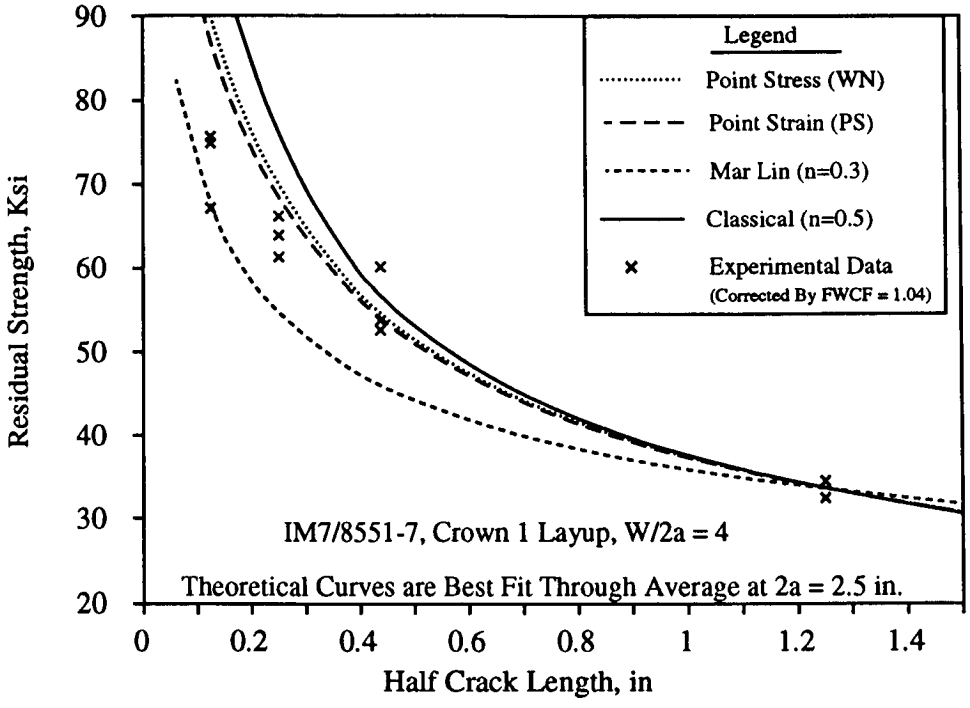

Figure 26: Comparison of IM7/8551-7 Experimental Results With Different Failure Criteria

Figure 27 shows results for the AS4/938 tape material and a Crown1 layup. Again the comparison is made for fracture parameters determined from the average strength data of the largest crack length. In this case, the ML criteria and a singularity of 0.3 compares well with the two largest crack lengths. In similar comparisons, most other materials and layups also compared best with the ML theory for larger crack sizes in which the singularity becomes dominant. Possible corrections to the ML theory using parameters similar to those in WN and PS (Ref. 34) would likely result in improved prediction of trends for small crack sizes.

As shown in Figure 28, the AS4/938 tape Crown2 laminate was one of the two cases in which a fracture theory compared well with the experimental data for the full crack length range. Unfortunately, specimens with 2.5 in. cracks were not tested for this layup, which limits the ability to judge the order of singularity. The IM6/937A Crown2 tape layup also compared well with the ML theory for cracks ranging from 0.25 in. to 0.875 in. Good correlations with the ML theory indicate a

constant H_c value. Although this was evident for small crack lengths and the Crown2 layup, it was not seen for other layups of either material type. The Crown1 laminate (results shown in Figure 27) had similar ply orientations as those used for Crown2.

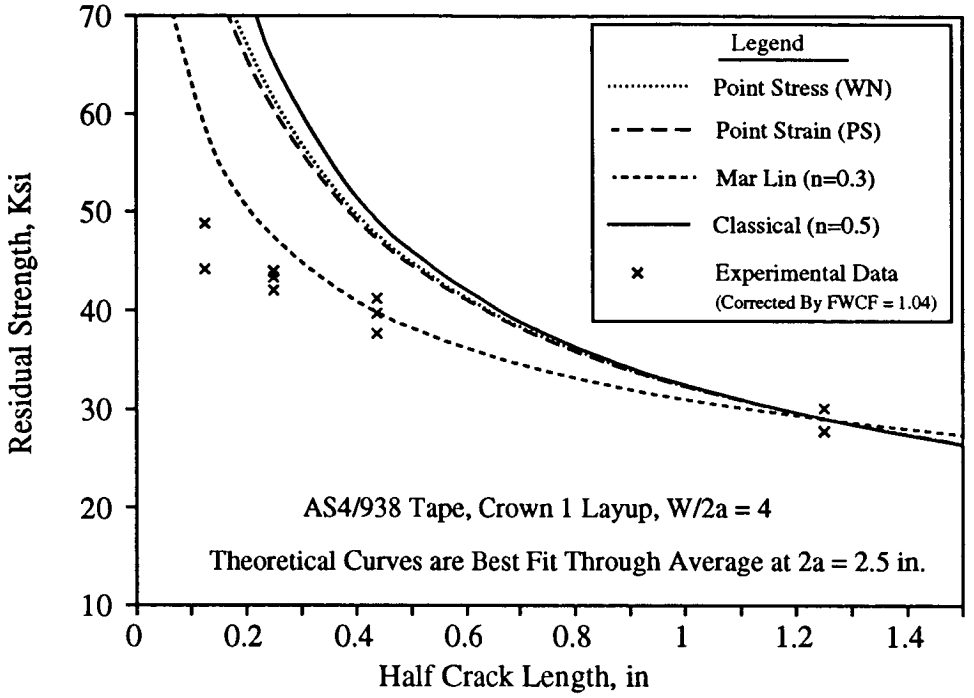

Figure 27: Comparison of AS4/938 Tape (10 Ply Laminate) Experimental Results With Different Failure Criteria

One unique feature of the Crown2 layup was that it had the largest number of plies of all laminates tested. A previous study with tape laminates (Ref. 9) showed that experimental values for the classical fracture toughness approached a constant value, independent of "small" crack lengths (i.e., ranging in size from 0.5 in. to 1.25 in.), for thick laminates that contain many plies. Perhaps laminate thickness relates to characteristics of composite materials that tend to change the small crack resistance.

Theoretical work discussed in the subsection entitled **"Review of Failure Criteria"** indicated that levels of inhomogeneity in a composite material microstructure can reduce the crack tip stress intensity (Refs. 28, 29, 30, 31). Conceivably, the inhomogeneous structure created in tape by the prepreg manufacturing processes (i.e., intralaminar regions of higher than average resin and fiber content) would become smeared as the number of plies increased. This is conceivable because fiber and resin rich regions of individual plies would tend to misalign as the number of plies increased in a hand layup process, yielding a more homogeneous inplane density distribution as laminate thickness increased. In the case of automated tow-placed laminates, a numerically controlled machine is more likely to repeat the placement of an inhomogeneous structure. This may explain why tow-placed laminates have higher fracture strengths (and associated fracture parameters) than tape laminates with the same constituents and layup.

Figure 29 shows theoretical comparisons with experimental data for the AS4/938 tow-placed Crown1 laminate. As shown in Figure 27 for AS4/938 tape material having the same laminate layup, the ML theory best represents the tow data in Figure 29. A close evaluation of the two figures indicates that

tow test results deviate further from the ML curve than does tape data. In addition to providing further evidence of the inability of the failure criteria to predict small crack effects, tape appears to be more notch sensitive than tow-placed laminates. Notch insensitivity suggests a higher level of inhomogeneity, reducing the stress concentration in the tow-placed laminates. The hypothesis posed in the previous paragraph may explain the manner in which this inhomogeneity is produced.

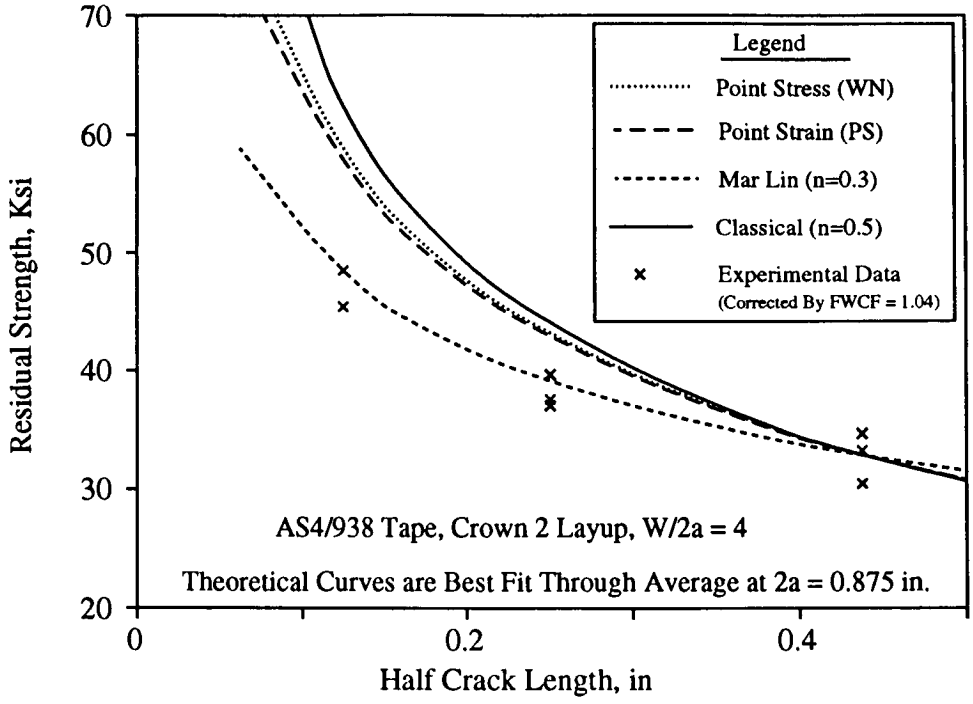

Figure 28: Comparison of AS4/938 Tape (16 Ply Laminate) Experimental Results With Different Failure Criteria

As used in the current discussions, the idea of inhomogeneous levels of microstructure relate to point-to-point changes in the laminate properties. For example, a level of inhomogeneity affecting tension fracture is perceived as inplane variations in laminate density and moduli that repeat as a function of a characteristic length. The pattern in which such variations repeat from point to point in a laminate is expected to depend on the manufacturing process, panel thickness, and fiber/matrix architecture.

Tow-placed intraply hybrid laminates are the most dramatic example of a material that has point-to-point inplane variations in properties. Figure 30 shows results for Hybrid #5 (consisting of bands of T1000 and AS4) that indicate strong deviations from theory for small crack sizes. There is no indication that the test results for a 2.5 in. crack are large enough to determine the proper singularity. For the range of cracks tested, all hybrids were found to be relatively notch insensitive as compared to tape laminates. These results suggest that this class of materials has significant changes in the stress intensity as a function of material architecture, notch size, and shape. Some form of generalized theory appears needed to help model the behavior exhibited by tow-placed hybrids.

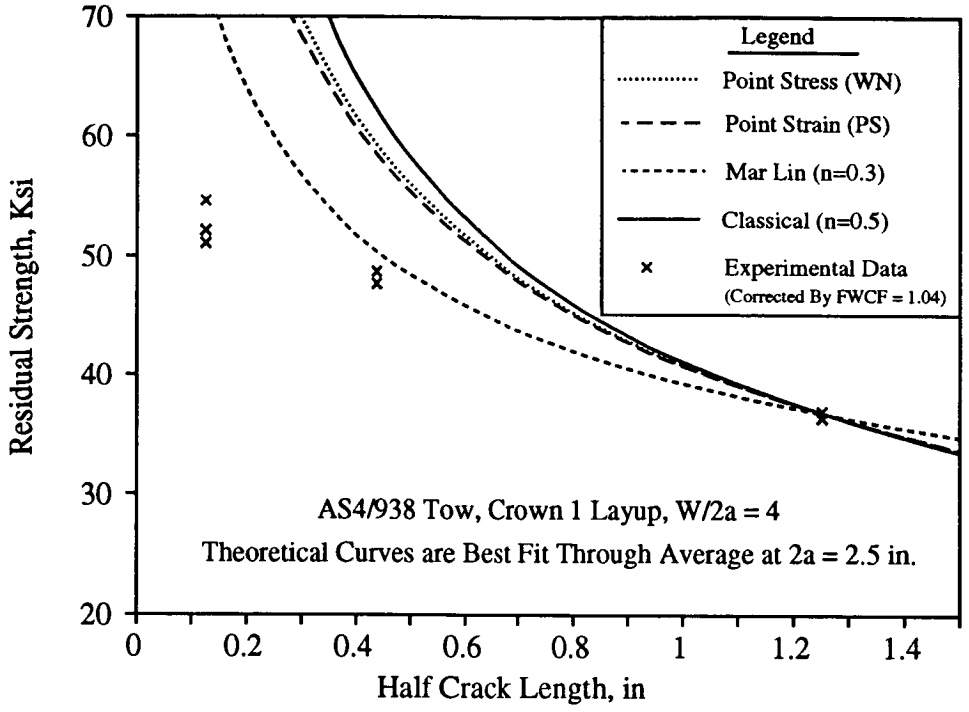

Figure 29: Comparison of AS4/938 Tow-Placed Laminate Experimental Results With Different Failure Criteria

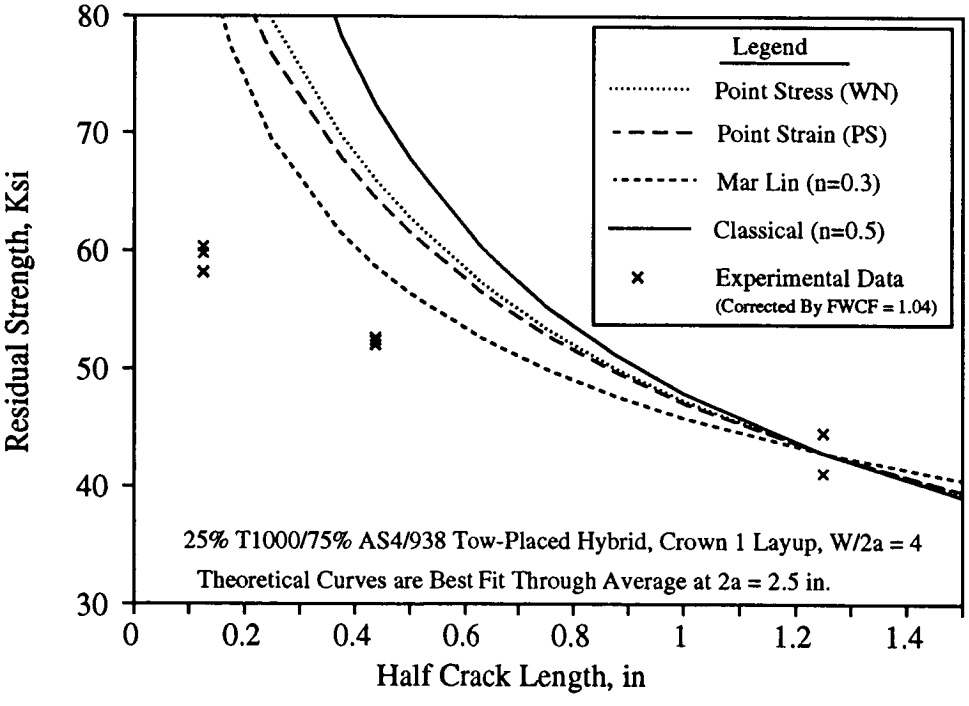

Figure 30: Comparison of AS4/T1000/938 Hybrid Tow-Placed Laminate Experimental Results With Different Failure Criteria

It is possible to estimate the order of singularity for all theories presented in this section by comparing changes in residual strength with crack size. During the course of discussions, it was suggested that such an exercise is best performed with the largest crack sizes in the data base. In an effort to evaluate the complete data set, the average 0.875 in. notched strength results were plotted versus those for 2.5 in. crack lengths. Each point in Figure 31 represents an average data pair for a specific material and layup (including angle and cross ply laminates). The majority of points fall between theoretical curves for $n = 0.1$ and 0.3. Linear regression analysis of all the data in Figure 31 yields a slope of 0.78, a small Y-intercept (1.77), and $R^2 = 0.82$. The corresponding singularity for this regression slope is $n = 0.24$.

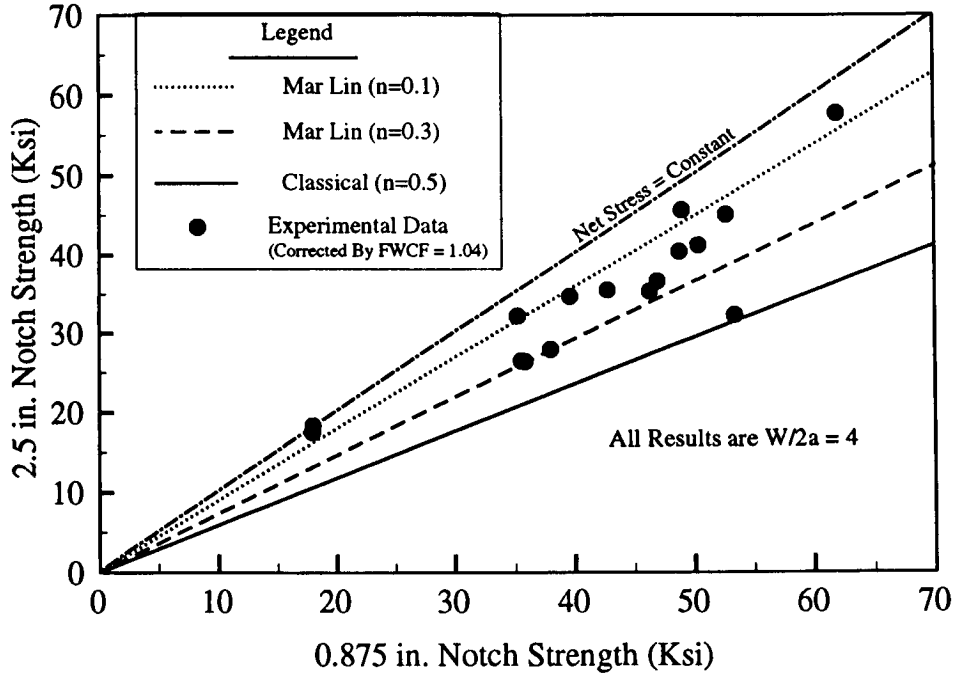

Figure 31: Evaluation of the Order of Singularity for All Laminates Having Both 0.875 in. and 2.5 in. Notched Strength Test Data

The single point in Figure 31 falling close to the $n = 0.5$ theoretical line corresponds to IM7/8551-7, which has the highest resistance to splitting. This, in combination with the $n = 0.3$ of the IM6/937A material, indicates that the singularity is not related to the idealized crack at the fiber/matrix interface. Theoretically, these two materials would have nearly identical singularities since the respective shear moduli and Poisson's ratios are very similar. The significant difference between these two materials, however, is the resin toughness, implying that the level of splitting may relate to the effective singularity.

Points in Figure 31 near the $n = 0.1$ line correspond to crossply and angleply tape laminates, and tow-placed hybrids that may still be under the influence of "small notch" effects. Crossply tape laminates and tow-placed hybrids undergo extensive matrix damage at the crack tip, including splitting. This is further evidence that splitting has the effect of reducing the stress intensity and effective singularity.

Limited evidence suggests a reduced singularity provides improved predictions of large-crack strengths. A previous NASA/Boeing fuselage contract (NAS1-17740, Ref. 4) tested small ($2a$ = 0.25 in., W = 1.5 in) and large ($2a$ = 12 in., W = 30 in.) flat unstiffened center-crack specimens of two laminates. The panels were fabricated from AS6[14]/2220-3[15] tape material (2220-3 resin is somewhat tougher than 938 but significantly more brittle than 8551-7). Figure 32 compares the data from the 16-ply quasi-isotropic panel with the PS, WN point stress and ML (n = 0.3) methods, all calibrated with the 0.25 in. data. The ML method slightly underpredicts the 12 in. data, with the other methods underpredicting by approximately 50%. Similar results were seen for the second laminate. Although this data is of differing $W/2a$ values and without intermediate crack sizes, comparable results are expected for constant $W/2a$ and other crack sizes.

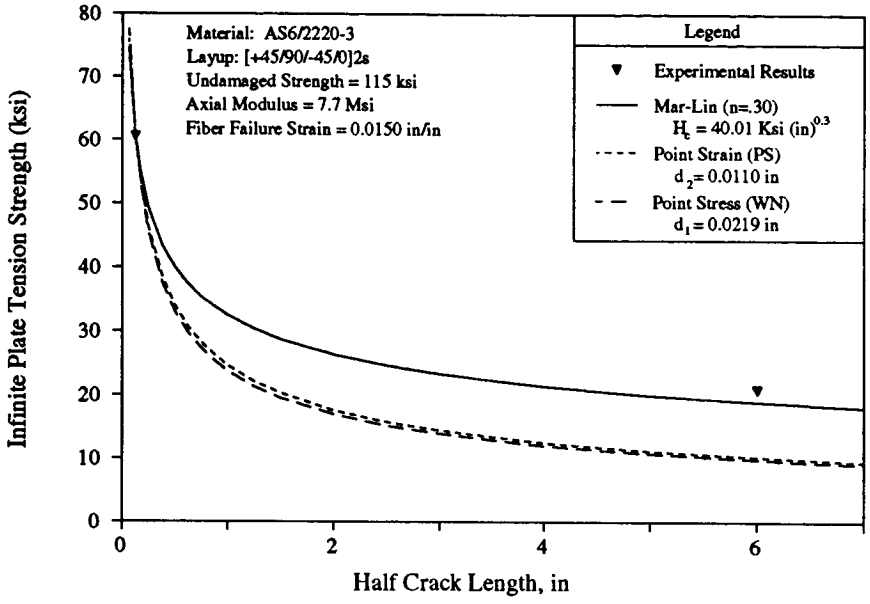

Figure 32: A Comparison of AS6/2220-3 Notched Strength Data and Three Fracture Models

In the past NASA contract (Ref. 4), the PS method was applied incorrectly to the data in Figure 32. The characteristic dimension associated with the WN point-*stress* method (d_1) obtained from the 0.25 in. data was used, and a good prediction of the 12 in. crack result was obtained merely by coincidence.

RECOMMENDED TEST PROCEDURES FOR FUSELAGE MATERIAL SCREENING

As previously discussed, the 0.25 in. open hole tension tests currently used for material screening does not provide meaningful information for predicting notched laminate strength for cracks on the order of several inches, nor is it likely to for larger cracks in configured structure. New procedures are therefore desired to screen materials for fuselage tension damage tolerance.

---

[14] AS6 is a graphite fiber system produced by Hercules, Inc.

[15] 2220-3 is a resin system produced by Hercules, Inc.

Selection of a specimen configuration is influenced by several factors.

- o The notch type (e.g., penetration versus machined crack) has a significant influence on the behavior.
- o Laminate thickness and layup also have significant influence on tension fracture performance.
- o Specimen strength depends on finite width effects that are not accurately modeled by classical methods; therefore, it is desirable to use $W/2a \geq 4$.
- o Grouping specimens of differing $W/2a$ values can artificially skew the strength versus crack-length curve.
- o Specimens with larger $W/2a$ values require additional material, and therefore cost, for a given crack length than do those with smaller $W/2a$ values.
- o Specimens wider than standard hydraulic grips (i.e., approximately 4 in.) require load introduction fixtures, resulting in increased test complexity and costs.

It is therefore recommended that all specimens be of center-crack configuration with $W/2a = 4$. This configuration can be used to test the notch type of interest and minimizes possible skewing of the notch sensitivity curve. In addition, the width of specimens having $W/2a = 4$ should reduce errors associated with classical finite width correction, while minimizing material and test costs for a given crack length. Fracture tests should be performed with specimen thickness and layups characteristic of the particular application.

A compromise for initial screening is to test at least 3 crack sizes ranging from 0.25 in. to approximately 1.0 in., all with $W/2a = 4$. The largest specimens are those having widths equal to the maximum allowed in hydraulic grips, typically in the 4.0 in. range. From this data, comparisons can be made with analysis to judge "small notch" effects and the apparent singularity. A second level of screening, using 10 in. wide coupons with 2.5 in. cracks, can be used to confirm trends for the most promising candidates from initial screening.

As part of the screening process, failure mechanisms should be studied to help evaluate material and laminate characteristics affecting fracture. For example, matrix splitting is one phenomenon that can effectively reduce the singularity and may be thought of as a material attribute for composite fuselage damage tolerance. Experimental measurements (e.g., crack opening displacements, pre-failure radiography) should be used to enhance visual observations.

The recommended test procedure listed in this section results in the most accurate extrapolations to large-crack tension fracture performance. Several materials tested in the current work were relatively notch insensitive, resulting in 2.5 in. crack data that may not indicate the effective singularity. An assumed singularity of 0.5 and the fracture toughness associated with the largest crack in the database will, at worst, yield conservative predictions of large-crack performance.

CONCLUSIONS

Collaborative efforts between Boeing and NASA have begun to address the issues associated with transport fuselage pressure damage tolerance. With all the composite material and laminate variables that can affect tension fracture performance, screening test and analysis procedures are needed to facilitate evaluations for fuselage applications. Tests involving 430 tension fracture specimens were performed in the current work to support ATCAS fuselage design and to develop a procedure for screening tension fracture performance. Requirements for screening tests included that the procedure

be economically feasible and recognize the effects of specimen geometry, analysis assumptions, and failure mechanisms.

Fracture tests were performed with ten candidate material types. These studies evaluated the effects of layup, notch type, specimen width, and notch size. As in past studies, large variations in notched strength were found due to layup. The strength for specimens with cracks and open holes of the same size (up to 0.875 in.) were within approximately 10% of each other, with no clear trend regarding the severity of one or the other. For a given layup, a ranking of materials based on the fracture strength of specimens with 0.25 in. cracks had no relationship with the performance observed for coupons with 2.5 in. cracks. This indicated the limits of current material screening tests involving a 0.25 in. open hole.

Material variables evaluated for tension fracture performance included fiber type, matrix toughness, and intraply hybridization of towpreg consisting of different fiber types. In addition, both hand layup tape and automated tow placement were considered as manufacturing variables for fabricating laminates. The IM6-fiber laminates provided a 5 to 25% increase in fracture strength over those consisting of AS4, compared to a 20 to 25% increase in fiber and unidirectional ply strength. Matrix toughness was found to have a major effect on increasing the notch sensitivity of the material. The toughened IM7/8551-7 material was 35% higher than IM6/937A at small cracks but 7% lower at 2.5 in. cracks. This was hypothesized to be due to the toughened materials resistance to matrix splitting. Matrix splits are believed to relieve the notched stress concentration and enhance tension fracture strength, particularly for large notches.

Tow-placed laminates were found to have 10 to 25% higher fracture strengths than tape consisting of the same volume of fiber and matrix constituents, and significantly reduced sensitivity to crack size. Hybrids consisting of AS4 and either S2-glass or T1000 graphite fibers had reduced notch sensitivity, similar to AS4 tow-placed laminates. Strengths of hybrids and non-hybrids segregate at large notch sizes, with an up to 17% increase in the former. This may relate to interactions between percent hybridizing fiber, hybrid repeat unit width, and notch size. Hybrids exhibited large amounts of matrix splitting and delamination prior to failure. The AS4/S2-glass hybrids also had significant post-failure load carrying capability.

The tension fracture performance of specimens with machined cracks and sharp penetrations created by an impact event were compared. The latter is more characteristic of the real damage threat. The instrumented impact response during the penetration event was found to depend on material and laminate variables. Post-impact damage levels and tension fracture performance were also found related to the same variables. In the case of the thickest laminates tested, the tension fracture strengths of specimens with impact penetrations were up to 20% higher than those for coupons with machined cracks. For the minimum thickness range of concern for fuselage structures (approximately 0.1 in.), the specimens with machined cracks had fracture strengths similar to those with impact penetrations. One notable exception was in the case of IM7/8551-7, which had post-impact tension fracture strengths that were 20% lower than those for specimens with machined cracks. Evidence suggests that impact penetration of IM7/8551-7 laminates may result in effective crack extension via fiber breakage.

Experimental data was used to evaluate finite width correction analysis and composite failure criteria. Comparison of finite width corrected data for specimens with the same crack lengths, but differing $W/2a$, indicated significant deviation. The finite width corrected strengths for specimens with $W/2a = 2$ were up to 30% less than those for $W/2a = 4$. In order to minimize this finite width effect, all failure criteria were evaluated using the variable crack length data for specimens having a constant $W/2a = 4$.

Failure criteria that were evaluated for accuracy in predicting the effect of notch size included three theories with the classical singularity of 0.5: LEFM, point stress, and point strain. Analysis using a singularity of 0.3 was also compared to experimental results. For most materials and layups in the database, each failure criteria was found to have fracture parameters that increased with increasing crack length over a range of small crack sizes (i.e., up to 1.0 in. long). With the exception of comparisons with LEFM, these findings differ from most past studies. Differences with past evaluations were discussed in the text including the method of determining an undamaged laminate strength and the correction of fracture data with variable *W/2a*.

Despite the noted inaccuracy, modified analysis methods that include "characteristic dimensions" are better at predicting small crack experimental trends than LEFM. This suggests the classical crack stress intensity is inaccurate for composites and that the actual distribution has characteristics that have an effect similar to the point stress and point strain formulations (i.e., stress intensity that is generally lower and a function of notch size). A hypothesis was posed based on evidence from analysis and experiments that suggest small crack stress distribution is strongly influenced by material inhomogeneity. Reductions in stress concentration occur for cracks having a length within several orders of magnitude of the material inhomogeneity scale. For a given crack size, therefore, notched strength increases with increasing scale of inhomogeneity. Possible scales of inhomogeneity include fiber diameter, tow width, and hybrid repeat unit width.

Each fracture theory converges to a curve dominated by the order of singularity at large crack sizes. Larger crack data (i.e., up to 2.5 in. long) for several materials and laminate layups tended to converge with failure criteria having a singularity of 0.3. One notable exception was the toughened material, IM7/8551-7, that tended to converge to the classical curve for singularity of 0.5. This and other evidence suggested that the effective singularity was dependent on matrix splitting. The ability to split and relieve the notch stress concentration relates to characteristics of the material and laminate layup.

FUTURE WORK

Several major efforts in the tension-fracture arena are targeted for continued work by ATCAS during 1991 and 1992. The major thrust in testing will be the verification of the crown panel design. These tests are outlined in Table 2. Testing of coupons with sizes on the order of specimens discussed in this paper will also continue, collecting data for additional laminates and addressing such issues as the relative strengths of holes and cracks at larger (i.e., 2.5 in.) sizes, increased strain rates, finite width effects, hybridization, and the role of material inhomogeneity. Work will be conducted with other contractors to understand the increased performance of the tow-placed material form, to enable control and maintenance of these improvements.

Curvature	Stiffening	Loading	Approximate Crack Size (in.)	Number of Specimens
flat	none	uniaxial	12	3
flat	none	biaxial	2.5	8
flat	tear straps	uniaxial	8	3
flat	hat stringers	uniaxial	14	2
curved	hoop tear straps	biaxial	20	1
curved	hat stringers, J frames	biaxial	25	3

Table 2: Crown Verification Testing

Analytically, efforts will focus on the further evaluation of predictive models for larger crack sizes, structural configurations, and curvature effects. In addition, work is planned in the development of analytical techniques for addressing the dynamic aspects of the pressure-release problem associated with an actual penetration of a transport fuselage.

Several suggestions for additional work, outside the scope of ATCAS, can be made based on findings in the current study. First, improved analysis methods are needed for predicting changes in small notch stress distribution as a function of notch geometry and material inhomogeneity. Experiments should be performed to separate the effects of material microstructure and progressive damage accumulation on local stress concentrations. The relationship between layup, material type, progressive damage accumulation, and the effective singularity for large notch sizes also needs to be studied. Some form of progressive damage models is needed for predicting the effects of panel width and matrix damage on stress concentration. Finally, experimental databases that include large crack sizes and combined loads for other composite materials are needed to best understand features that affect tension damage tolerance. The limited results found to date suggest a wide range of composite material performance, with the most attractive candidates having tension fracture properties better than traditional metal materials used in transport fuselage.

ACKNOWLEDGEMENTS

The authors would like to express their appreciation to Brian Coxon (Intec, Inc.), Dodd Grande (Boeing Materials Technology), and Fu-Kuo Chang (Stanford University) for the efforts in specimen testing and evaluation of failure mechanisms.

REFERENCES

1. Ilcewicz, L. B., Smith, P. J., Walker, T. H., and Johnson, R. W., "Advanced Technology Commercial Fuselage Structure," First NASA Advanced Composites Technology Conference, NASA CP-3104, Part 1, pp. 127-155, 1991.

2. Swanson, G. D., Ilcewicz, L. B., Walker, T. H., Graesser, D., Tuttle, M., and Zabinsky, Z., "Local Design Optimization for Transport Fuselage Crown Panels," in Proceedings of Ninth DoD/NASA/FAA Conference on Fibrous Composites in Structural Design, NASA CP- , 19 . (Paper of this compilation.)

3. Awerbuch, J., and Madhukar, M. S., "Notched Strength of Composite Laminates: Predictions and Experiments -- A Review," J. of Reinforced Plastics and Composites, Vol. 4, pp. 1-159, 1985.

4. Smith, P. J., Thomson, L. W., and Wilson, R. D., "Development of Pressure Containment and Damage Tolerance Technology for Composite Fuselage Structures in Large Transport Aircraft," NASA CR-3996, 1986.

5. Kim, J. K., and Mai, Y. W., "High Strength, High Fracture Toughness Fibre Composites with Interface Control - A Review," Composites Science and Technology, Vol. 41, pp. 333-378, 1991.

6. Kennedy, J. M., "Damage Tolerance of Woven Graphite/Epoxy Buffer Strip Panels," NASA TM 102702, 1990.

7. Poe, C. C., Jr., and Kennedy, J. M., "An Assessment of Buffer Strips for Improving Damage Tolerance of Composite Laminates," Journal of Composite Materials Supplement, Vol. 14, pp. 57-70, 1980.

8. Harris, C. E., and Morris, D. H., "Fractographic Investigation of the Influence of Stacking Sequence on the Strength of Notched Laminated Composites," in Fractography of Modern Engineering Materials: Composites and Metals, ASTM STP 948, pp. 131-153, 1987.

9. Harris, C. E., and Morris, D. H., "Effect of Laminate Thickness and Specimen Configuration on the Fracture of Laminated Composites," Composite Materials Testing and Design (Seventh Conference), ASTM STP 893, pp. 177-195, 1986.

10. Lagace, P. A., "Notch Sensitivity and Stacking Sequence of Laminated Composites," Composite Materials Testing and Design (Seventh Conference), ASTM STP 893, pp. 161-176, 1986.

11. Daniel, I. M., Rowlands, R. E., and Whiteside, J. B., "Effects of Material and Stacking Sequence on Behavior of Composite Plates with Holes," Experimental Mechanics, Vol. 14, pp. 1-9, 1974.

12. Walter, R. W., Johnson, R. W., June, R. R., and McCarty, J. E., "Designing for Integrity in Long-Life Composite Aircraft Structures," Fatigue of Filamentary Composite Materials, ASTM STP 636, pp. 228-247, 1977.

13. Aronsson, C. G., "Stacking Sequence Effects on Fracture of Notched Carbon Fibre/Epoxy Composites," Composites Science and Technology, Vol. 24, pp. 179-198, 1985.

14. Poe, C. C., Jr., "Fracture Toughness of Fibrous Composite Materials," NASA Technical Paper 2370, 1984.

15. Ilcewicz, L. B., Dost, E. F., McCool, J. W., and Grande, D. H., "Matrix Cracking in Composite Laminates With Resin Rich Interlaminar Layers," in Proc. of 3rd Symposium for Composite Materials: Fatigue and Fracture, ASTM STP 1110, 1991.

16. Wang, A. S. D., Reddy, E. S., and Zhong, Y., "Three-Dimensional Simulation of Crack Growth in Notched Laminates," J. of Reinforced Plastics and Composites, Vol. 9, pp. 134-150, 1990.

17. Box, G. E. P., Hunter, W. G., and Hunter, J. S., Statistics for Experimenters, John Wiley & Sons, Inc, 1978.

18. Konish, H. J., Jr., "Mode I Stress Intensity Factors for Symmetrically-Cracked Orthotropic Strips," in Fracture Mechanics of Composites, ASTM STP 593, American Society for Testing and Materials, pp. 99-116, 1975.

19. Tan, S. C., "Finite-Width Correction Factors for Anisotropic Plate Containing a Central Opening," J. of Composite Materials, Vol. 22, pp. 1080-1097, 1988.

20. Whitney, J. M. and Nuismer, R. J., "Stress Fracture Criteria for Laminated Composites Containing Stress Concentrations," J. Composite Materials, Vol. 8, pp. 253-265, 1974.

21. Nuismer, R. J. and Whitney, J. M., "Uniaxial Failure of Composite Laminates Containing Stress Concentrations," in Fracture Mechanics of Composites, ASTM STP 593, American Society of Testing and Materials, pp. 117-142 (1975).

22. Pipes, R. B., Wetherhold, R. C., and Gillespie, J. W., Jr., "Notched Strength of Composite Materials," J. Composite Materials, Vol. 12, pp. 148-160, 1979.

23. Pipes, R. B., Gillsespie, J. W., Jr. and Wetherhold, R. C. "Superposition of the Notched Strength of Composite Laminates," Polymer Engineering and Science, Vol. 19, No. 16, pp. 1151-1155, 1979.

24. Tan, S. C., "Notched Strength Prediction and Design of Laminated Composites Under In-Plane Loadings," J. of Composite Materials, Vol. 21, pp. 750-780, 1987.

25. Poe, C. C., Jr. and Sova, J. A., "Fracture Toughness of Boron/Aluminum Laminates with Various Proportions of 0° and ±45° Plies," NASA Technical Paper 1707, 1980.

26. Poe, C. C., Jr., "A Unifying Strain Criterion for Fracture of Fibrous Composite Laminates," Engineering Fracture Mechanics, Vol. 17, No. 2, pp. 153-171, 1983.

27. Waddoups, M. E., Eisenmann, J. R., and Kaminski, B. E., "Macroscopic Fracture Mechanics of Advanced Composite Materials," J. Composite Materials, Vol. 5, pp. 446-454, 1971.

28. Chiang, C. R., "Inhomogeneity Effect on the Stress Intensity Factor," J. Composite Materials, Vol. 21, pp. 610-618, 1987.

29. Ilcewicz, L. B., Shaar, C., Kennedy, T. C., and Wilson, J. B., "Experimental Evidence of a Relationship Between Ultrasonic Wave Dispersion and Fracture," Engineering Fracture Mechanics, Vol. 26, pp. 895-908, 1986.

30. Nakamura, S. and Lakes, R. S., "Finite Element Analysis of Stress Concentration Around a Blunt Crack in a Cosserat Elastic Solid," Computer Methods in Applied Mechanics and Engineering, Vol. 66, pp. 257-266, 1988.

31. Eringen, A. C., Speziale, C. G., and Kim, B. S., "Crack-Tip Problem in Nonlocal Elasticity," J. Mech. Phys. Solids, Vol. 25, pp. 339-355, 1977.

32. Mar, J. W. and Lin, K. Y., "Fracture Mechanics Correlation for Tensile Failure of Filamentary Composites with Holes," Journal of Aircraft, Vol. 14, No. 7, pp. 703-704, 1977.

33. Lin, K. Y. and Mar, J. W., "Finite Element Analysis of Stress Intensity Factors for Cracks at a Bi-Material Interface," Int. J. of Fracture, Vol. 12, No. 2, pp. 521-531, 1987.

34. Tsai, H. C., and Arocho, A. M., "A New Approximate Fracture Mechanics Analysis Methodology for Composites with a Crack or Hole," Report NADC-88118-60, 1990.

35. Aronsson, C. G., and Backlund, J., "Tensile Fracture of Laminates with Cracks," J. Composite Materials, Vol. 20, pp. 287-307, 1986.

36. Aronsson, C. G., and Backlund, J., "Damage Mechanics Analysis of Matrix Effects in Notched Laminates," in Composite Materials: Fatigue and Fracture, ASTM STP 907, pp. 134-157, 1986.

37. Chang, F. K., and Chang, K. Y., "A Progressive Damage Model for Laminated Composites Containing Stress Concentrations," J. Composite Materials, Vol. 21, pp. 834-855, 1987.

38. Chamis, C. C., "Computational Simulation of Progressive Fracture in Fiber Composites," NASA TM-87341, 1986.

39. Barenblatt, G. I., "The Mathematical Theory of Equilibrium Cracks in Brittle Fracture," Advances in Applied Mechanics (Edited by Dryden, H.L. and von Karman, T.), Vol. 7, pp. 55-129, 1962.

40. Swanson, S. R., and Christoforou, A. P., "Response of Quasi-Isotropic Carbon/Epoxy Laminates to Biaxial Stress," J. Composite Materials, Vol. 20, pp. 457-471, 1986.

41. Chamis, C. C., and Sinclair, J. H., "Micromechanics of Intraply Hybrid Composites: Elastic and Thermal Properties," NASA-TM-79253, 1979.